

THE CARNIAN PLUVIAL EVENT IN THE TOFANE AREA (CORTINA D'AMPEZZO, DOLOMITES, ITALY)

Anna Breda¹, Nereo Preto^{1,2}, Guido Roghi², Stefano Furin³, Renata Meneguolo^{1,4}, Eugenio Ragazzi⁵, Paolo Fedele⁶, Piero Gianolla³.

With 24 figures

¹ Department of Geosciences, University of Padova, Italy;

² Institute of Geosciences and Earth Resources, CNR, Padova, Italy;

³ Department of Earth Science, University of Ferrara, Italy;

⁴ StatoilHydro ASA, Stavanger, Norway;

⁵ Department of Pharmacology, University of Padova, Italy;

⁶ Museo delle Regole, Cortina D'Ampezzo.

Introduction

What happened at the end of the Early Carnian, some 235–230 million years ago? All over the Dolomites, the lower–upper Carnian transition is evident from the distance as a break between the majestic rock walls of the massive Cassian Dolomite and those of the well bedded Dolomia Principale. This morphological step is strikingly evident, for example, all around the Sella Platform, and locally evolved to extended plateaus, as below the Tre Cime di Lavaredo or at Lagazuoi, north of Passo Falzarego. Even the slopes of Col Gallina and Nuvolau, uniformly dipping northward toward Passo Falzarego, are structural surfaces representing the exhumed platform top of the demised lower Carnian Cassian Dolomite (Fig. 1). And here our excursion starts.

The aim of this field trip is twofold.

On the one hand, evidence will be shown of a climatic swing from arid, to humid, and back to arid climate in the Carnian of the Tofane area. We here denote the whole climatic episode, regardless of its polyphase nature, as the “Carnian Pluvial Event”.

On the other hand, the effects of this climatic event on sedimentation and biota will be illustrated, from the km scale of carbonate platform geometries to the smaller scale of facies associations and lithologies. The morphological features of famous mountain groups of the Dolomites, as depicted above, are a direct consequence of the sedimentary turnover triggered by the Carnian Pluvial Event.

The locality we have chosen for this purpose is the area at the foot of the Tofane mountains, with the sections at Passo Falzarego and Rifugio Dibona, the last one probably the best exposed and complete section encompassing the Carnian Pluvial Event (Fig. 1). The Tofane mountains face the “conca di Cortina”, at the heart of the Dolomites, a paradise for mountain lovers. We hope to convince you that this is also a paradise for earth scientists.

THE CARNIAN PLUVIAL EVENT

The term “Carnian Pluvial Event” denotes an episode of increased rainfall which had a well recognizable and widespread influence on Carnian marine and continental sedimentary systems. Its onset is da-

ted to the latest Early Carnian (Julian), by ammonoid and conodont biostratigraphy (Fig. 2). Initially identified as one of the major turnovers in the stratigraphic evolution of the Northern Calcareous Alps (the “Reingrabener Wende” of Schlager and Schöllnberger, 1974), it was then interpreted as a shift towards

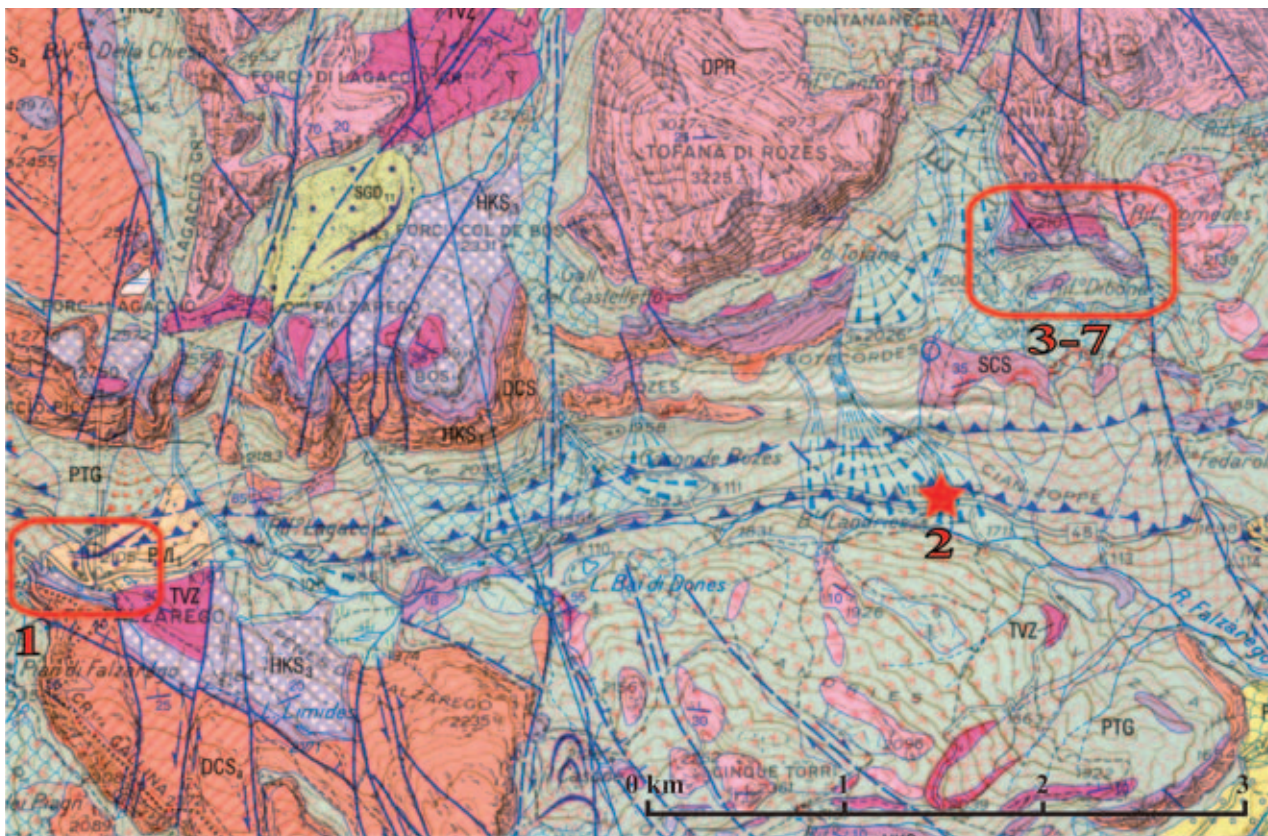


Fig. 1: Location of stops and geology of the Passo Falzarego - Tofane - Rif. Dibona area. DCS (peach-colored): Cassian Dolomite, Lower Carnian carbonate platform; SCS (Lilac, red dots): San Cassiano Formation, Lower Carnian basinal marls and calcarenites; HKS (various colors): Heiligkreuz Formation, Lower-Upper Carnian mixed sedimentation; TVZ (purple): Travenanzes Formation, Upper Carnian alluvial plain to carbonate lagoon; DPR (pink): Dolomia Principale/Hauptdolomit, Upper Carnian - Norian carbonate tidal flat and lagoon. Geological map 1:50000 (from Neri et al. 2007, modified).

humid climate (Carnian Pluvial Episode of Simms and Ruffell, 1989).

In the area of this field trip, the Carnian Pluvial Event had a strong impact on virtually all aspects of sedimentation.

- The best evidence for a climate episode comes from the study of paleosols (Fig. 3). During the Carnian Pluvial Event, paleosols forming in this region were associated with well developed paleokarst, and by the formation of histic and spodic horizons. All these features require a positive water budget throughout the year, and are generally missing in paleosols formed before and after the event (see Paleosol box).

- As in most parts of the Tethys and Europe, the Carnian Pluvial Event is here marked by the sudden input of coarse siliciclastics, which we attribute to increased rainfall and runoff. Arenites and conglomerates often contain plant debris, testifying for a

well developed vegetation cover. Palynological assemblages within plant-bearing arenites and shales show xerophytic elements associated with highly diversified hygrophytic elements (see Pollen box).

- Amber that occurs in millimetre-sized droplets is abundant in sediments deposited during the Carnian Pluvial Event (see Amber box).

- The growth of the Early Carnian rimmed carbonate platforms was suddenly interrupted, similarly to what occurred in the Northern Calcareous Alps (Reingrabener Wende, Schlager and Schöllnberger, 1974). After the demise of the Early Carnian platforms (Keim et al., 2001), depositional geometries switched to ramp (Preto and Hinnov, 2003; Bosellini et al., 2003) and carbonate production recovered fully only with the onset of the Dolomia Principale (Gianolla et al., 2003).

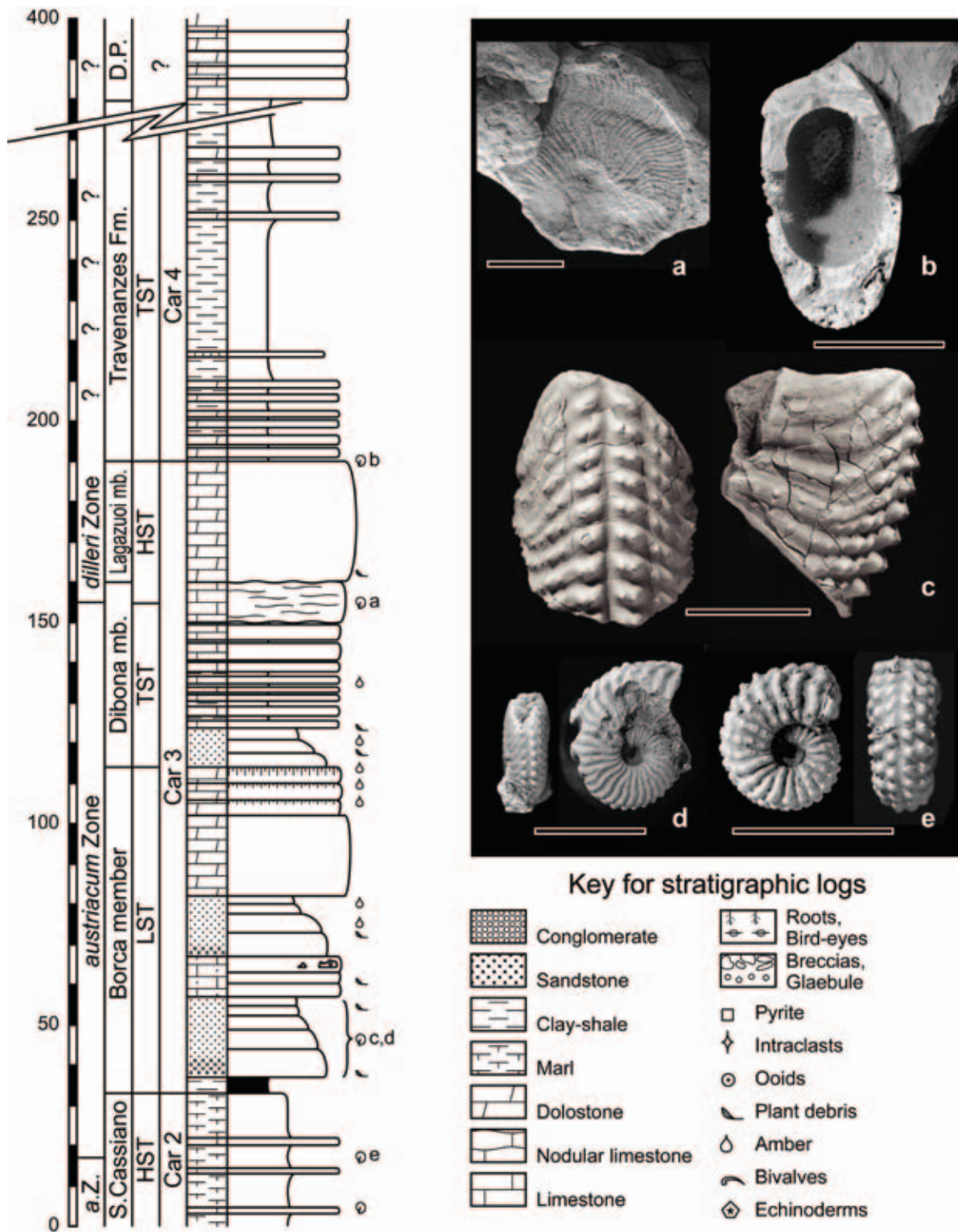


Fig. 2: Composite synthetic stratigraphic section of the Heiligkreuz and Travenanzes Formations in basal settings of the Cortina area. D.P. = Dolomia Principale. Thickness in metres. a.Z. = *aonoides* Zone; V. = Vallandro Member; HST = Highstand Systems Tract; TST = Transgressive Systems Tract; LST = Lowstand Systems Tract. Some significant ammonoids are also illustrated. a) *Shastites* cf. *pilari* (Hauer), Col dei Bos (West of Rif. Dibona), Upper Dibona member, *dilleri* Zone. Other well preserved specimens of this species, collected from the same horizon but in different localities, are illustrated by De Zanche et al. (2000). b) cf. *Jovites* sp., Col dei Bos (West of Rif. Dibona), upper Lagazuoi member, *dilleri* Zone. c) cf. *Austrotrachyceras* sp., Rif. Dibona, Borca member, *austriacum* Zone. d) *Sirenites senticosus* (Dittmar), Rumerlo (East of Rif. Dibona), Borca member, *austriacum* Zone. e) *Sirenites betulinus* (Mojsisovics), Boa Staolin (Cortina d'Ampezzo), upper San Cassiano Fm., *aonoides* VS *austriacum* Zone. Scale bars = 1 cm.

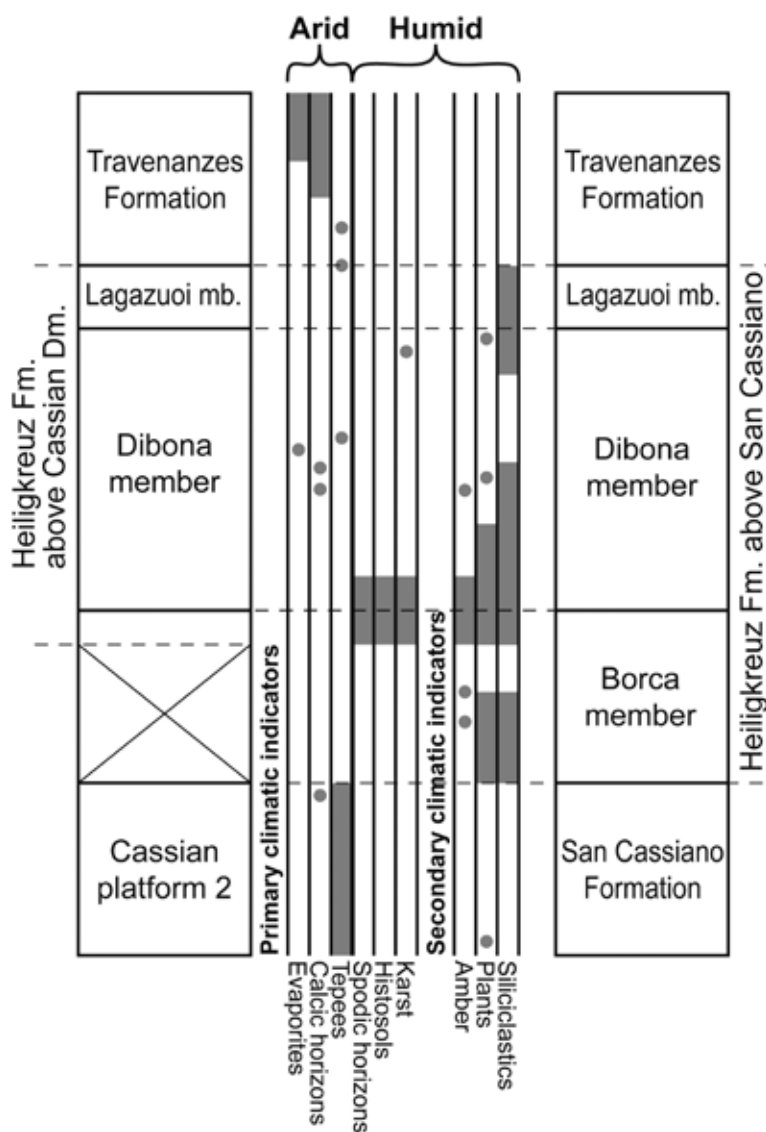


Fig. 3: Distribution of climatic indicators in the Cassian Dolomite, Heiligkreuz Fm. and Travenanzes Fm. This compilation is based on several localities of the central-eastern Dolomites including Rifugio Dibona. Gray bars indicate common occurrences; gray circles indicate isolated occurrences. Humid climate indicators are concentrated within the lower Heiligkreuz Fm.; a complex organization of the climate pulse with at least three more humid sub-pulses can be hypothesized.

GEOLOGICAL SETTING

The Dolomites are part of the Southern Alps, a structural domain of the Alps characterized by south to south-east vergent thrusts and folds, and by the absence of Alpine metamorphism. Within the Southern Alps, the Dolomites are a ca. 35 km large pop-up structure (Castellarin and Doglioni, 1985). Alpine deformation is mostly confined outside the pop-up, thus, the Dolomites constitute a low-strain

domain: Alpine thrusts are present, but produced relatively minor dislocations and did not obliterate completely pre-Alpine tectonics.

A volcanic and sedimentary succession, encompassing a stratigraphic interval from the lower Permian to the Tertiary, and lying on a Variscan metamorphic basement, is documented in the Dolomites (Fig. 4). The stratigraphic interval relevant to this field trip is the Carnian (Upper Triassic). During the Upper Triassic, this region was located in a north tropical paleolatitude as suggested by the samples collected some 5-6 km west of Passo Falzarego, in the basinal Wengen and San Cassiano formations, where the GSSP candidate of the Ladinian-Carnian Boundary at Stuores has been suggested (Broglia Loriga et al., 1999).

The Cassian Dolomite

The lower Carnian (Julian) starts with the growth of rimmed carbonate platforms (Leonardi, 1968; Bosellini, 1984), isolated in some cases, as for the Sella Platform connected with a continental area in other cases (Bosellini et al., 2003). Two generations of rimmed carbonate platforms, represented by Cassian Dolomite 1 and 2 (cf. De Zanche et al., 1993) were prograding onto the basins of the S. Cassiano Fm., some hundreds of meters deep (Fig. 5). The distribution of basinal areas was mainly controlled by the position and shape of carbonate buildups (Fig. 6). The S. Cassiano Fm. is composed of marls and shales with intercalated carbonate turbidites and oozes shed from nearby platforms.

Cassian platforms are often intensely dolomitized; nevertheless, depositional geometries are recognizable and at least two facies associations can be distinguished in the field: the inner platform and the slopes (Gianolla et al., 2008).

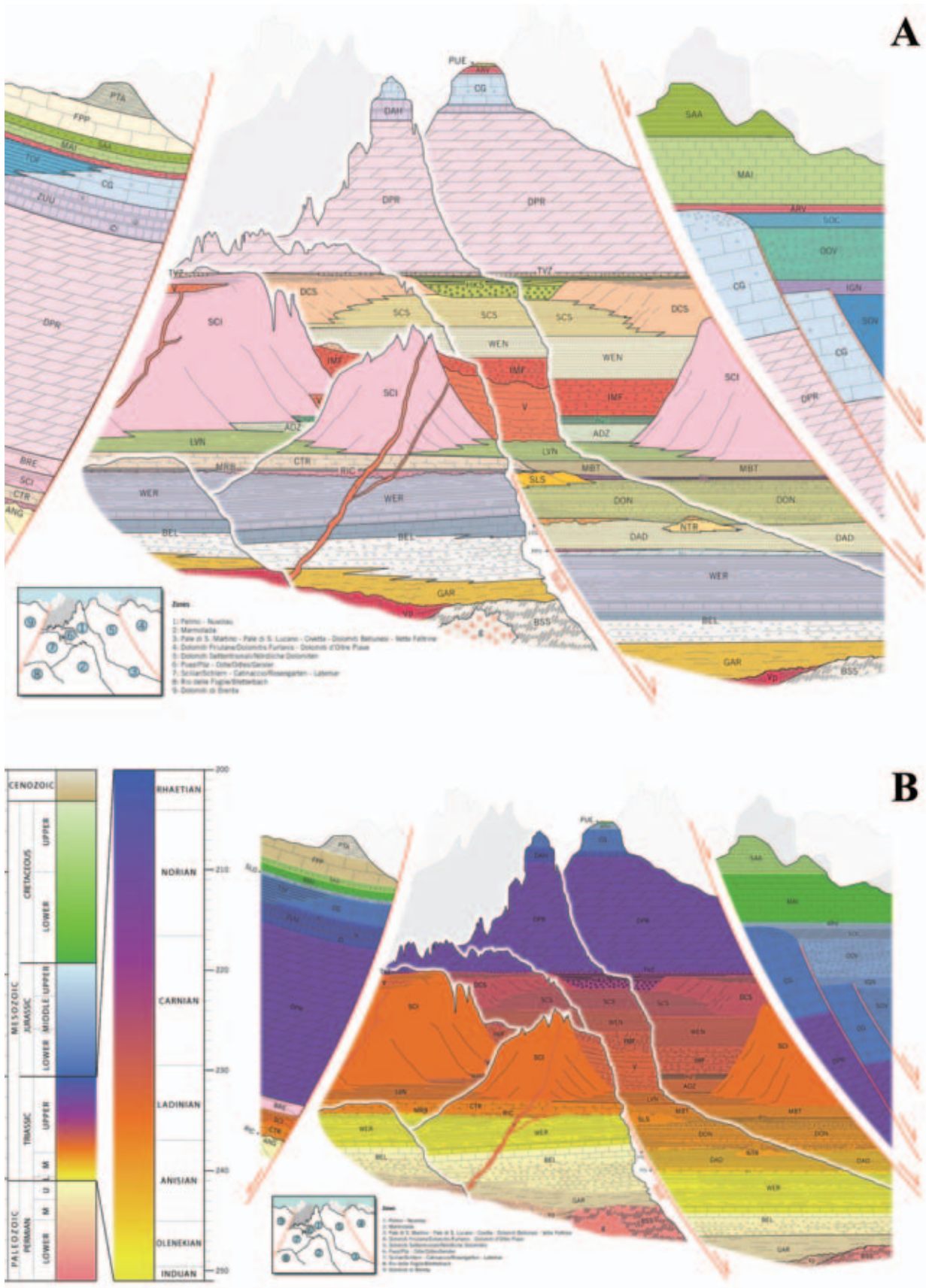


Fig. 4: Lithostratigraphic (A) and chronostratigraphic (B) framework of the Dolomites and surrounding areas (from Gianolla et al., 2008). s a

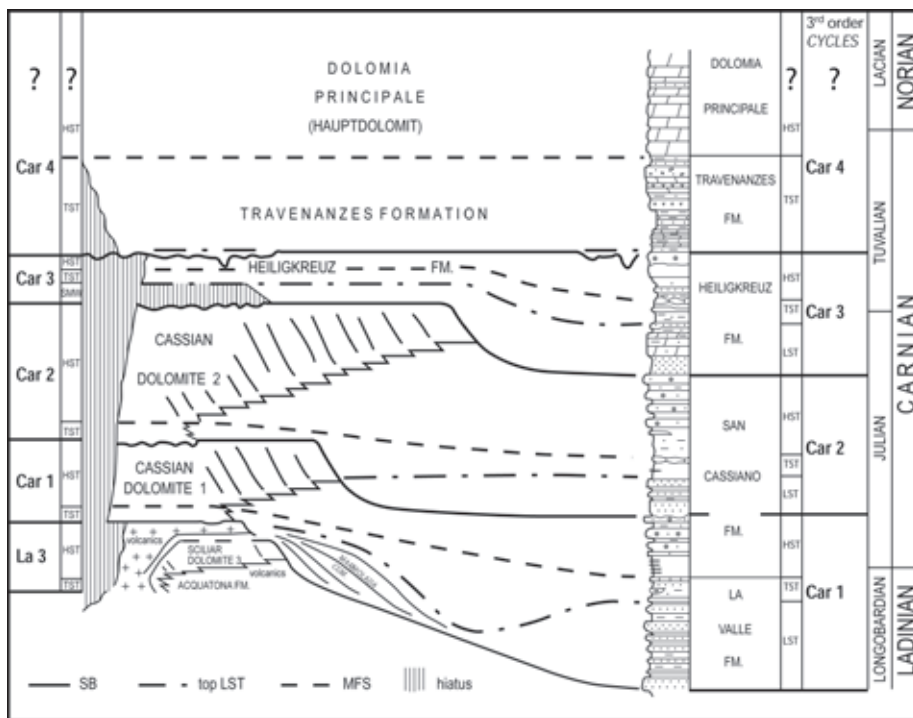


Fig. 5: Detail of the Carnian stratigraphy of the Dolomites. From De Zanche et al. (1993), modified.

Slopes are recognized by their prominent clinoforms, dipping up to 30–35° and tangentially joining the basins. Most common facies are grainstones and megabreccias, with boulders often composed of microbialitic boundstones rich in early marine cements, originated at platform margins and/or upper slopes (Gianolla et al., 2008).

The platform margin is narrow and its facies association is rarely recognizable (Keim and Schlager, 2001) because of dolomitization.

The platform interior consists of metre-scale peritidal sedimentary cycles with fine-grained fossiliferous carbonates (dolomites with large gastropods, bivalve moulds, heads of colonial corals) of subtidal environment, alternating with metre-scale tepees, pisolitic beds and stromatolitic laminites indicating supratidal deposition.

Tetrapod footprints, including those of small dinosaurs, are common in the southern sector where platforms were probably attached to an emerged land (Avanzini et al., 2000).

The Heiligkreuz Formation

The articulated topography outlined by the Cassian platforms began to flatten out during the latest Julian (Early Carnian) with the infilling of the basins which were, at this point, only a few hundreds of meters deep. Cassian platforms are characterized by climbing progradation geometries and clinoforms become less steep. With the deposition of the Heiligkreuz Formation (ex Dürrenstein Fm. auctorum) this infilling phase is completed (Fig. 7).

The Heiligkreuz Fm. is subdivided into three members (Neri et al., 2007) that document suc-

cessive filling phases of the remaining Cassian basins and record the crisis of rimmed carbonate platforms. The Borca member (HKS1) documents the first phase of basin infilling. It comprises dolomitic limestones, arenaceous dolomites and well-stratified hybrid arenites with abundant pelitic intervals. Locally large-scale cross bedding is recognized (as at Rif. Dibona). At the base boundstones with sponges, stromatoporphs and colonial corals are present in places (Member a in Russo et al., 1991), followed by bioturbated dolostones/dolomitic limestones with a benthic mollusk fauna. At the top well-stratified, light-gray to whitish dolomites with centimeter thick intercalations of black, gray or greenish marls, often arranged in peritidal cycles with stromatolitic horizons and topped by paleosols predominate.

This member is followed by the Dibona Sandstones member (HKS2), characterized by polymict conglomerates, dark, cross-bedded sandstones, brown, gray or blackish pelites, with frequent oolitic-bioclastic packstone-grainstone beds. Plant remains are present represented by centimeter-thick levels of coal and/or structured plant remains. Marine benthic fauna is abundant and differentiated, and associated with isolated remains of marine and terrestrial vertebra-

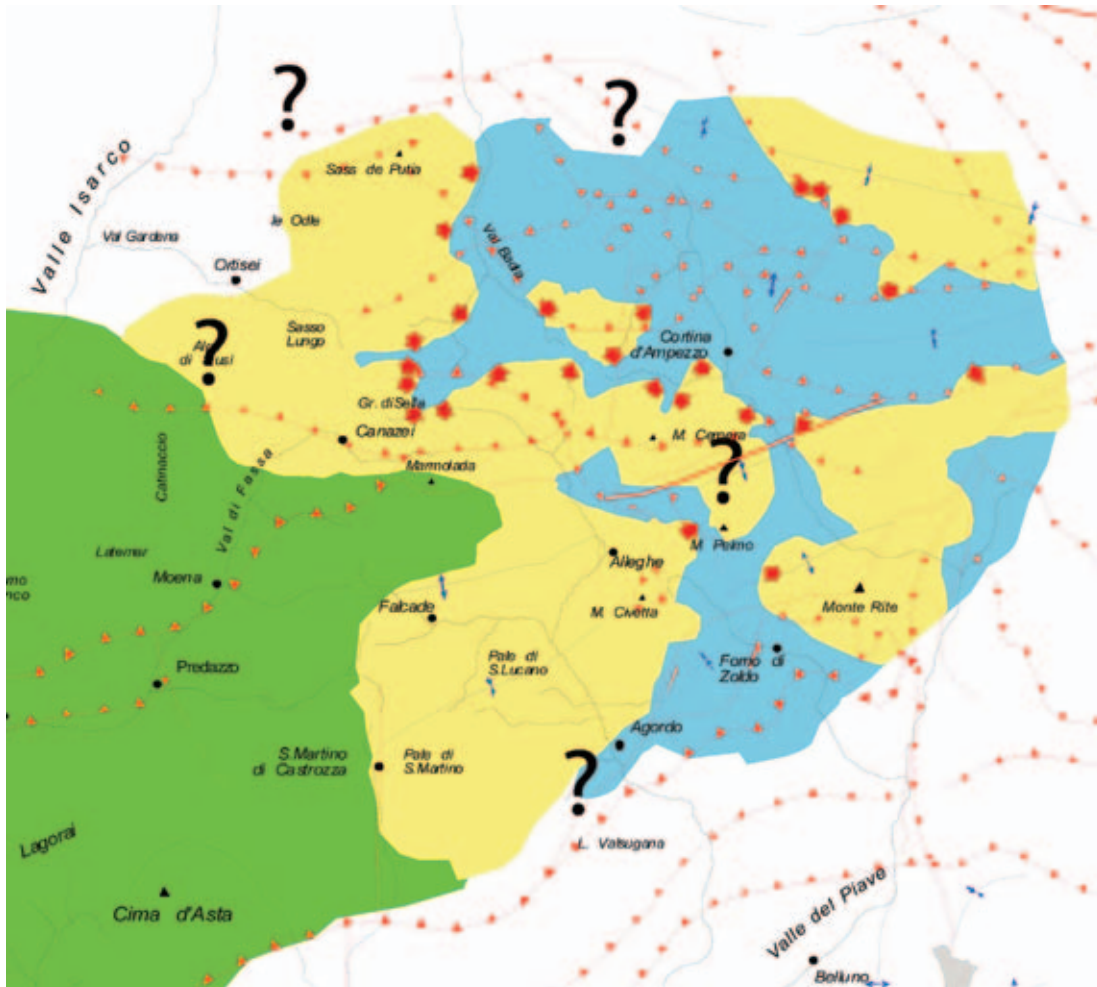


Fig. 6: Paleogeography of the Dolomites at the maximum development of the lower Carnian Cassian platforms. Green: emerged land; yellow: Cassian carbonate platform (red arrows indicate clinoform dip); light blue: San Cassiano Fm. (basin). Passo Falzarego (immediately west of Cortina d'Ampezzo) is located in a narrow intraplatform basin between the Lagazuoi-Tofane isolated platform and the Averau-Nuvolau block, connected to emerged lands.

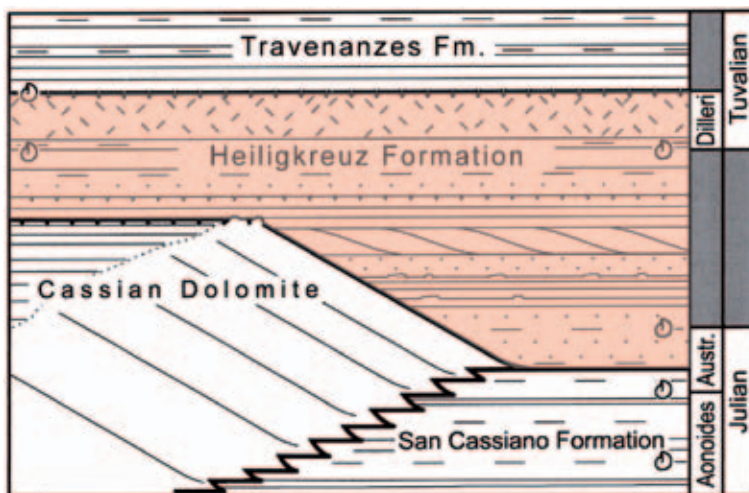


Fig. 7: Simplified stratigraphic setting of the Heiligkreuz Fm. (pink shading) in the Cortina area. The infilling of the inherited lower Carnian San Cassiano basin is completed already with the prograding shoal barrier and lagoon at the top of the Borca member (from Preto and Hinnov, 2003, modified).

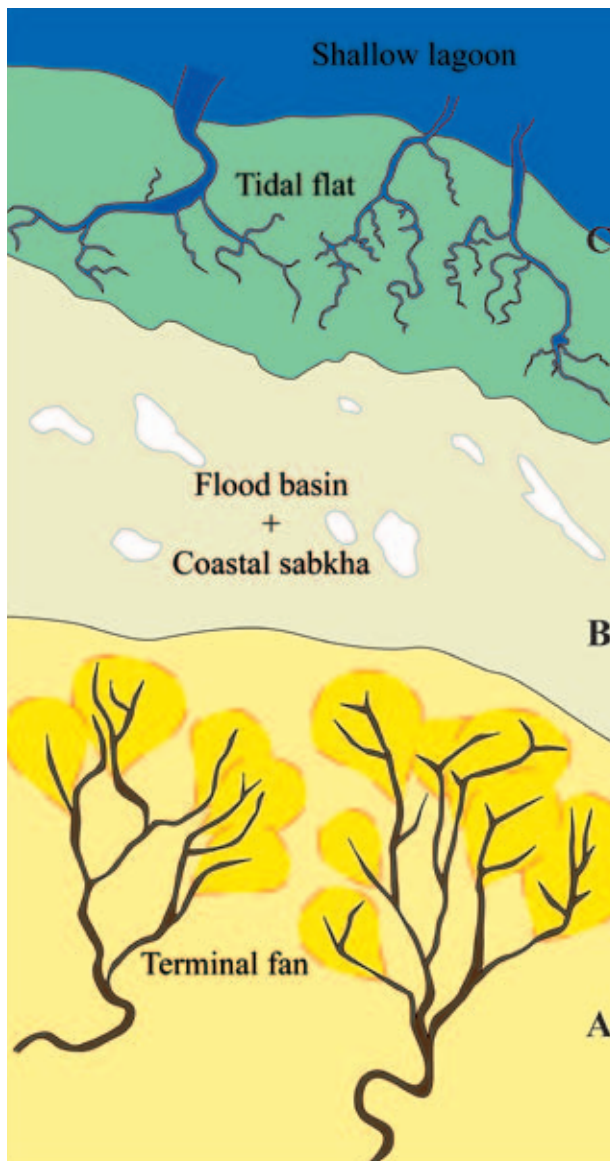


Fig. 8: Tentative reconstruction of the marginal depositional environments of the Travenanzes Fm. highlighting the interfingering among the A) terminal fan, B) flood basin (with coastal sabkha), and C) carbonate tidal flat + shallow lagoon environments. From Breda and Preto, 2008, modified.

tes. Amber is particularly abundant at the top of this member as well as at the top of the Borca member (see Amber box).

Finally, the Heiligkreuz Fm. is topped by the strongly dolomitized oolitic-bioclastic grainstones of the Lagazuoi member (HKS3). This unit is correlative to the Portella Dolomite of the Julian Alps (De Zanche et al., 2000; Preto et al., 2005). Locally, as at Passo Falzarego, this member is substituted by cross-bedded hybrid arenites (Falzarego Sandstones). With the deposition of the Lagazuoi member the paleotopography of the area was finally flattened.

The Travenanzes Formation

In the Late Carnian (Tuvalian) the subsequent depositional system represented by the Travenanzes Formation (ex Raibl Fm. auctorum) and by the Dolomia Principale records the return to mainly arid or semi-arid conditions and formed on a flat surface with a minimal topographical gradient (Breda and Preto, 2008).

The Travenanzes Fm. is a terrestrial to shallow-marine, mixed siliciclastic-carbonate succession (Bosellini et al., 1996; Neri et al., 2007). Deposition took place on a low-gradient coastal area fed by sediments originating from highlands located southwards, and opened to the north-northeast to the Tethys Ocean.

In the study area the Travenanzes Fm. consists of almost 200 m of aphanitic and crystalline dolostones, multicoloured mudstones with sandstone to conglomerate intercalations, and evaporitic intervals. Facies analysis and paleoenvironmental interpretation suggest the interfingering of alluvial plain, flood basin, and shallow lagoon deposits (Fig. 8), and a transition from continental to marine facies belts in a northerly direction.

The continental portion of this depositional system is constituted by an alluvial environment of terminal fan type (Kelly and Olsen, 1993) characterized by dominantly fine-grained floodplain mudstones with scattered, laterally-migrating conglomerate channels passing downslope to small ephemeral streams and sheetflood sandstones, and vanishing in a muddy flood basin. The association of calcic and vertic paleosols (see Paleosols box) indicates a semiarid to arid climate with seasonal precipitation or strongly intermittent discharge.

The flood basin is a low-lying coastal mudflat at the transition between terrestrial and marine deposition. Mudstones were deposited as suspension load during the temporary inundation of the (otherwise emerged) flood basin, both by sea water during storm surges and by the major river floods. Due to the dominantly arid climate the flood basin became the ideal site for evaporite deposition with the local development of a coastal sabkha.

The marine portion of this depositional system is constituted by carbonate tidal-flat and shallow-lagoon deposition characterized by aphanitic dolomites, granular dolostones rich in bivalves (Megalo-dontida) in growth position, foraminifera and diffuse bioturbation, algal-laminated and marly dolostones, with subordinate intercalations of prevalently dark mudstones and shales. Peritidal dolostones are at places indistinguishable from those of the overlying

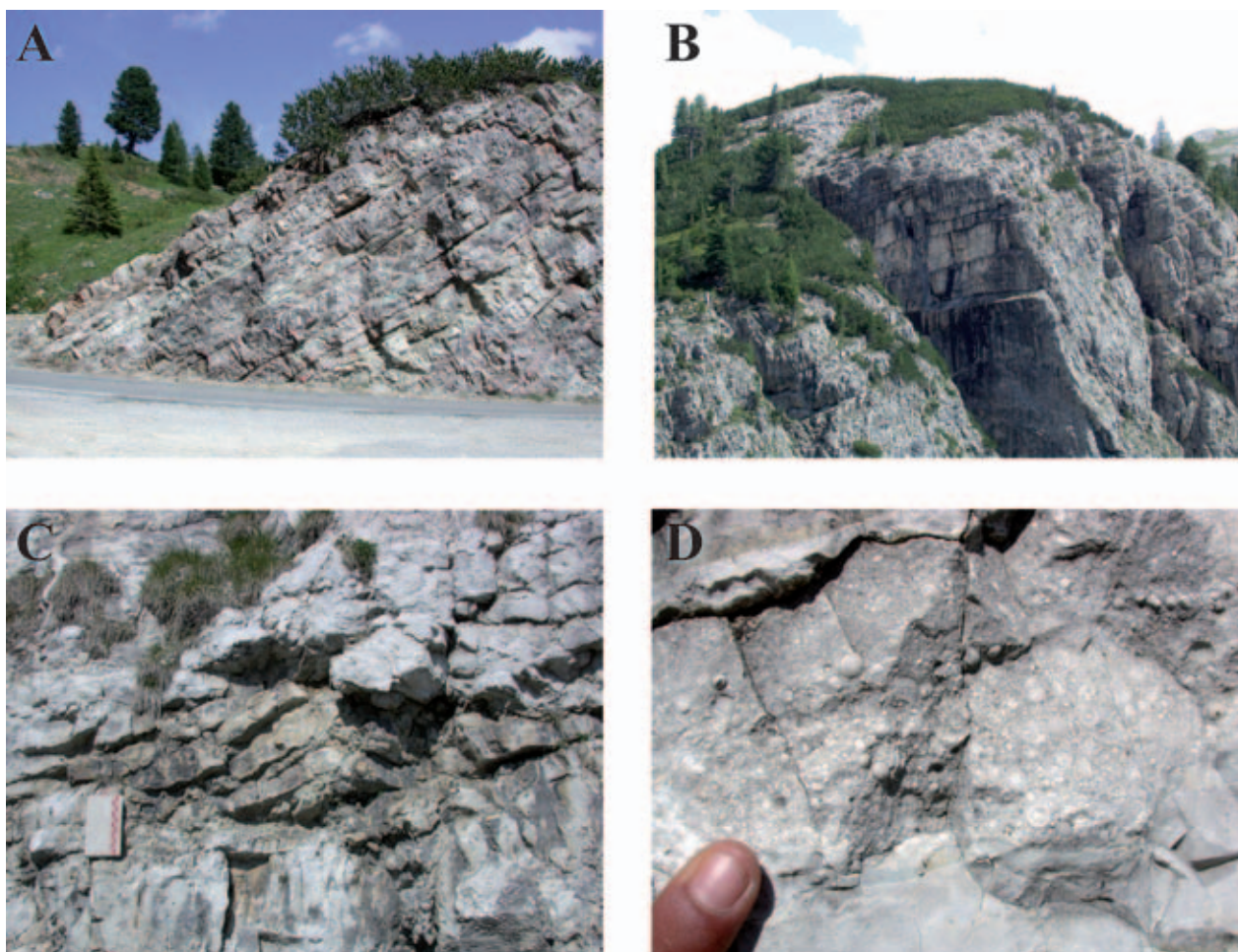


Fig. 9: Outcrop views of the Cassian Dm. (lower Carnian) at Passo Falzarego. A) top of the platform interior succession; above, the Heiligkreuz Fm. is poorly exposed; B) platform interior succession towards Col Gallina, with an evident upward decrease of bed thickness; C) tepee structure; D) marine pisoids within tepee cavity.

Dolomia Principale (Rossi, 1964; Bosellini, 1967; Bosellini and Hardie, 1988; Neri et al., 2007).

The Dolomia Principale

Near the end of the Tuvolian (Late Carnian) an important transgression in concomitance with a gradual climatic change to dryer conditions produced the southward migration of the shoreline and the disappearance of the terrigenous input, marking the onset of the Dolomia Principale peritidal deposition (Gianolla et al., 1998a). The onset of the broad peritidal environments that will characterize the Southern Alps for several million years is associated with more homogeneous subsidence trends and with the general restoration of shallow-water carbonate sedimentation also in those areas that were emerged for long time.

DESCRIPTION OF OUTCROPS

1. Cassian platform interior (lower Carnian) at Passo Falzarego

The excursion will start from the lower Carnian of Passo Falzarego and will proceed in stratigraphic order. The topic of the first stop is the characterization of the subaerial exposure surfaces within the uppermost Cassian Dolomite, immediately before its demise.

Passo Falzarego stays between a steep wall to the north and a relatively gently dipping slope to the south. This morphological arrangement is structurally controlled. Bedding dips uniformly to the north in the area, but the succession is dislocated by a major

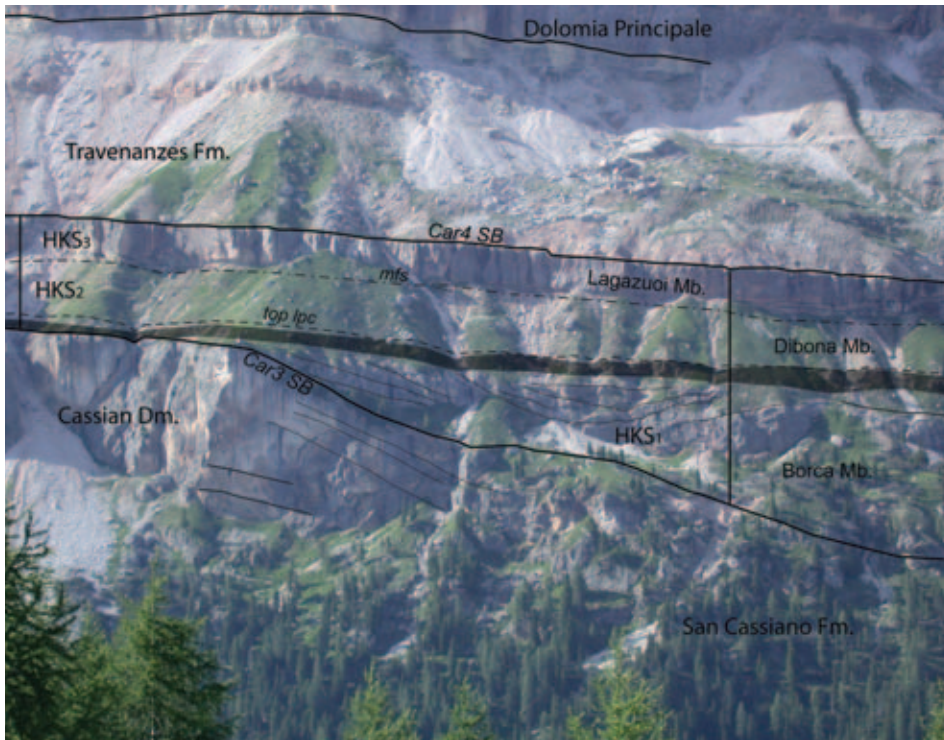


Fig. 10: Onlap of the Heiligkreuz Fm. on the slope of the second Cassian platform as seen from Cinque Torri. The Cassian platform is completely dolomitized; however, the reef zone is easily identified from the depositional geometries. The light dolomite unit (colored in grey) onlapping the slope is the prograding oolitic-bioclastic shoal of the upper Borca member (See stops 3-4); the tabular, massive dolomite ledge is the Lagazuoi member (from Stefani et al., 2004; Neri et al., 2007; Gianolla et al., 2008; modified).

south-vergent Alpine thrust that uplifted the north block (hanging wall) for about 700 m. The stratigraphic succession outcropping at the pass (2105 m asl) is thus repeated - with some significant variations - at Rifugio Lagazuoi (2750 m asl) at the terminal of the cabin lift.

Right SW of Passo Falzarego, along the main road, the platform top of the Cassian Dolomite is particularly well exposed (Fig. 9A, B). This succession was referred to the "Dürrenstein Dolomite" in the older geological literature (cf. Bosellini et al., 1982, 1996; Neri and Stefani, 1998) and was thought to onlap the slopes of a lower Carnian platform. Later investigations demonstrated that it corresponds to the platform interior of the Cassian Dolomite.

The succession is characterized by peritidal sedimentary cycles capped by subaerial exposure surfaces associated with tepee structures (Fig. 9C). Marine pisoids (Fig. 9D) are commonly found in tepee cavities and intra-tepee pools. A thinning-upward trend in the thickness of the sedimentary cycles indicates a progressive decrease in accommodation. Calcisols characterized by irregular micritic glaebules, pisoids with micritic core and thin micritic-sparitic coating, and laminated carbonate crusts occur towards the top of the succession (Baccelle and Grandesso, 1989). Platform sedimentation ended abruptly and a

palaeokarst breccia developed on the top of the peritidal succession (Stefani et al., 2004).

Above sedimentation started again with the deposition of the Dibona Sandstones member (HKS2 Heiligkreuz Fm.) which is, however, poorly exposed. At Passo Falzarego the upper Heiligkreuz Fm. is represented by arenites with planar bedding, and cross-bedding including herringbone cross-bedding, indicative of a shoreface environment with strong influence of tidal currents (Bosellini et al., 1978, 1982). This siliciclastic body is limited to the Passo Falzarego and its surroundings (Preto & Hinnow, 2003; Neri et al., 2007) and is correlative to the massive dolomites of the Lagazuoi member, clearly visible at Rifugio Lagazuoi on top of the wall north of the pass.

2. Depositional geometries of the Cassian platforms and Heiligkreuz Fm. from Rio Bianco

In this brief stop we will review the depositional geometries of the lower Carnian Cassian platforms and of the Heiligkreuz Fm., and thus the switch from rimmed platforms to ramp (Preto and Hinnov, 2003; Bosellini et al., 2003). The best perspective for these observations is from the Cinque Torri. Two generations of carbonate platforms (Cassian Dm. 1 and 2)

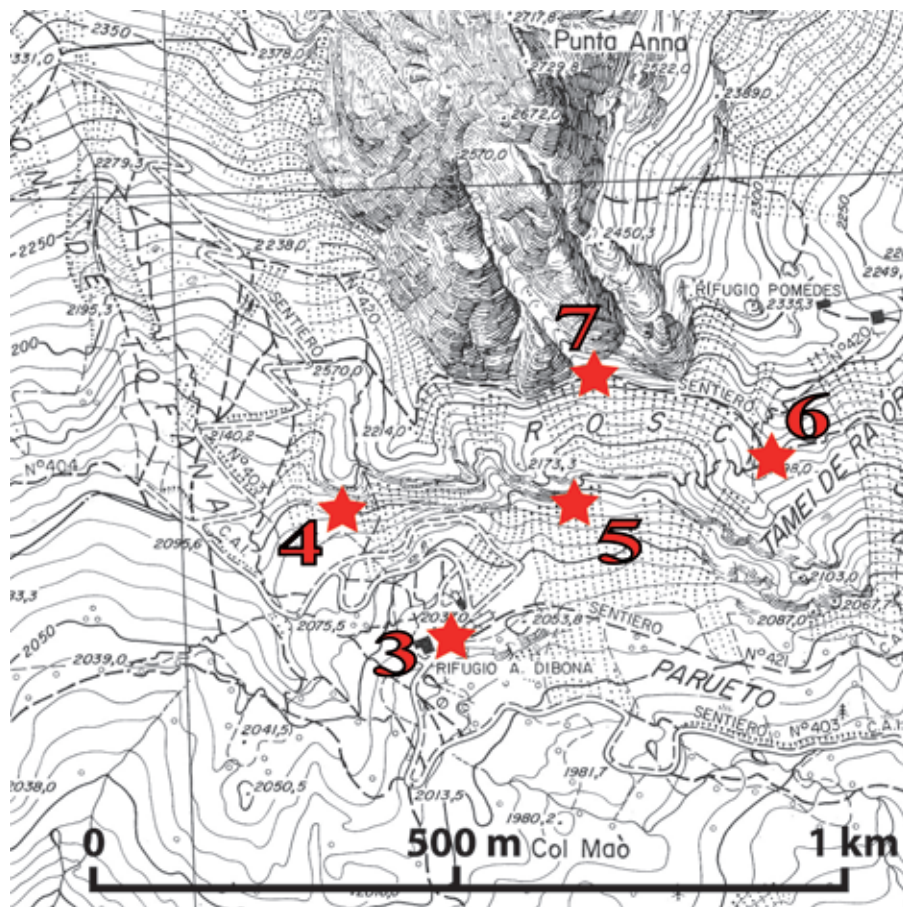


Fig. 11: Stops at Rifugio Dibona (CTR topographic map 1:10000, Regione Veneto, modified)

can be recognized, with the Heiligkreuz Fm onlapping the slope of the second Cassian platform (Fig. 10).

3. The Rifugio Dibona section: overview (Fig. 11)

The Rifugio Dibona section (Cortina d'Ampezzo, Belluno) presents expanded thickness and the more complete stratigraphic record of the region due to its position above the basinal setting where the San Cassiano Formation was deposited. This implies that sediments deposited immediately after the demise of the lower Carnian Cassian platform and that bypassed the platform top and slopes, i.e. lower and middle Borca member of the Heiligkreuz Fm. are preserved here (Figs. 7, 12).

Rifugio Dibona is a key section for the Carnian stratigraphy displaying an almost complete section of the Heiligkreuz Fm., the whole Travenanzes Fm. (here almost 200 m thick), and the Dolomia Principale (Figs. 2, 12). Thanks to the fairly continuous record of paleosols from the middle Heiligkreuz Fm.

upwards, the Rifugio Dibona section is ideal for the study of paleoclimatic trends and their relationship with sedimentation.

The Heiligkreuz Fm. crops out on the south faces of rock towers separated by narrow incisions (Fig. 13). Each incision corresponds to a nearly vertical fault uplifting the western block. The lowest part of the series is thus found to the west (left, facing the mountainside, Fig. 13A) while the uppermost part is more accessible to the east (i.e., right, Fig. 13C). Above, the Travenanzes Fm. breaks the slope ("via ferrata Cengia Astaldi"), and the Dolomia Principale constitutes the walls of Punta Anna (2731 m asl).

The most striking feature of the section, as seen from the distance, is a sedimentary body of dolostones with approximately 30 m high clinoforms dipping to the east (Fig. 13B). This unit is comprised in the upper Borca member and represents an oolitic-bioclastic shoal bordering a carbonate lagoon heavily polluted by terrigenous input (well layered white dolomite beds visible immediately above). This shoal is supposed to prograde above a middle-ramp environment characterized by frequent deposition of mass flows.

4. The middle Borca member

This outcrop is located in the westernmost block above Rifugio Dibona, and exposes the lowest part of the section just below the clinostratified dolostone unit (Fig. 14). The lower boundary of the clinoforms is not exposed here, but it was observed in a less accessible section some 750 m to the east.

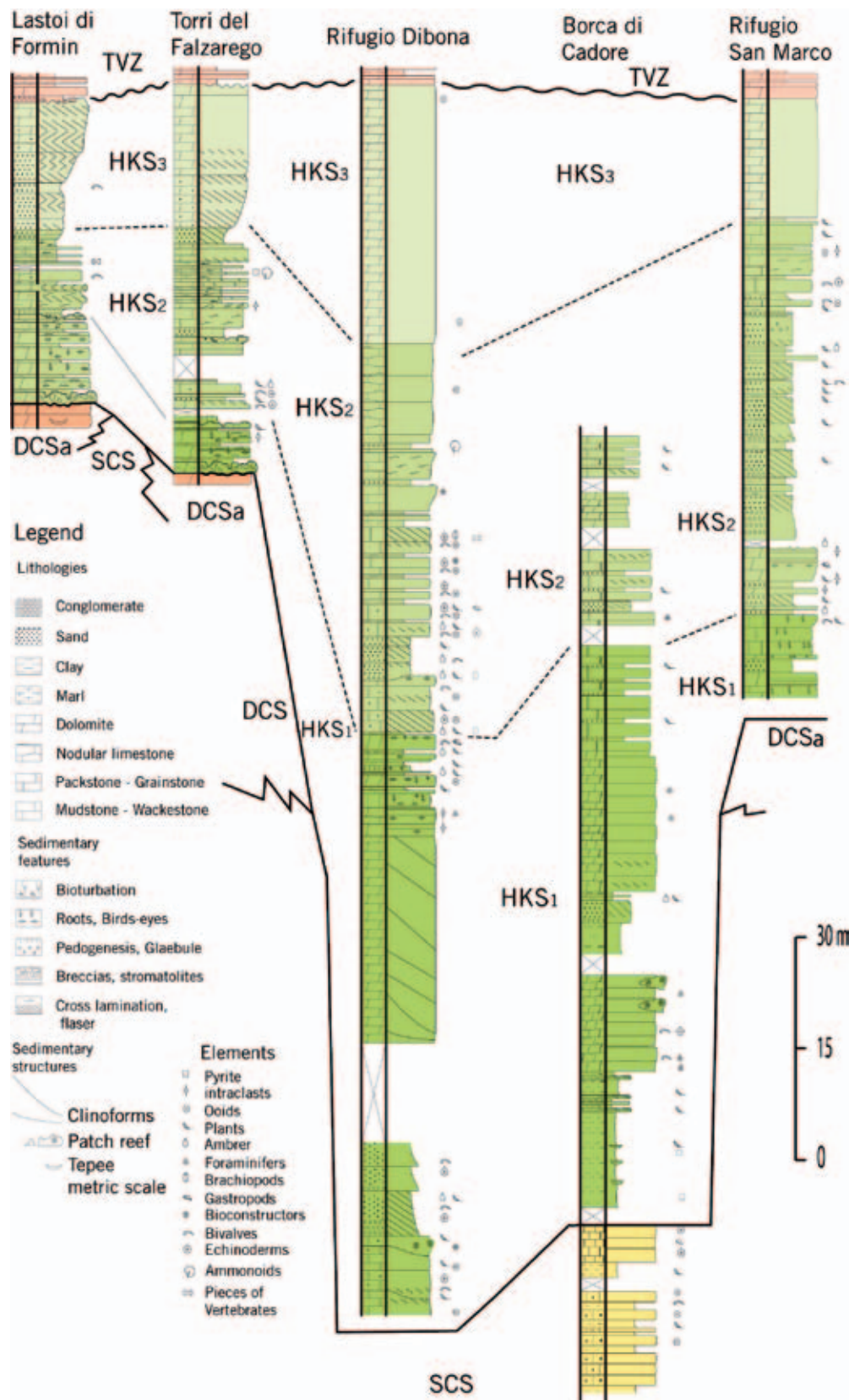


Fig. 12: Rifugio Dibona section (Heiligkreuz Fm.) and correlation with other sections in the central Dolomites. SCS: San Cassiano Fm.; DCS: Cassian Dolomite; HKS1: Borca member; HKS2: Dibona Sandstones member; HKS3: Lagazuoi member; TVZ: Travenanzes Fm. (from Preto and Hinnov, 2003; Stefani et al., 2004; Neri et al., 2007, modified).

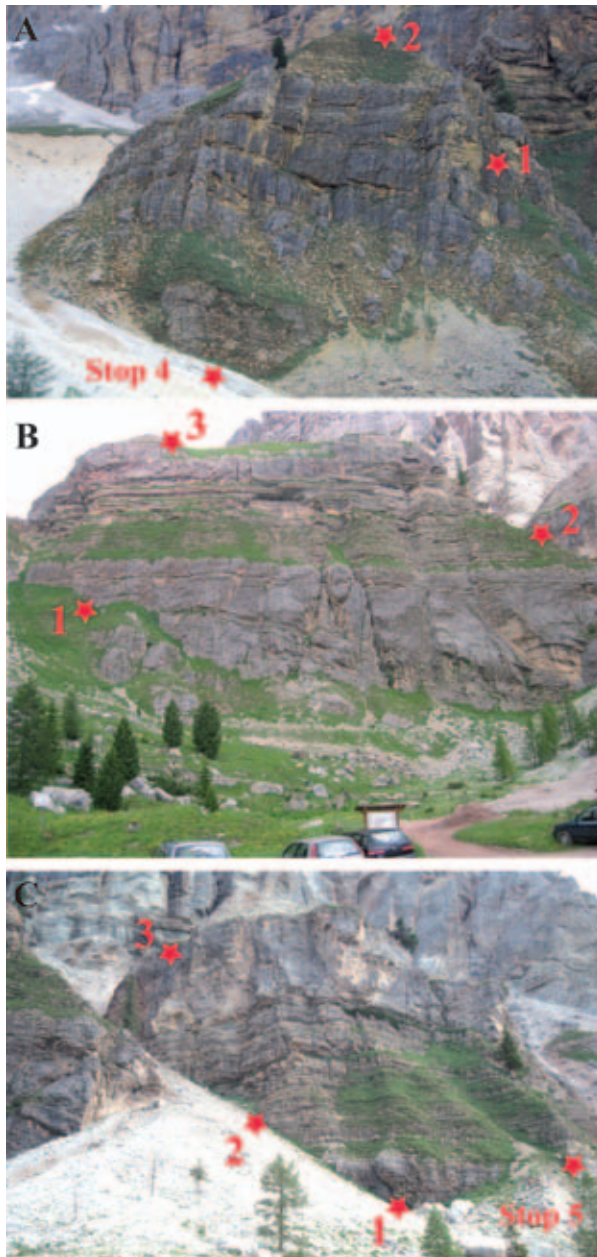


Fig. 13: Views of the Heiligkreuz Fm. from Rifugio Dibona. 1: Borca member, dolomitized prograding shoal barrier; 2: Dibona Sandstones member; 3: Lagazuoi member. A) The clinostratified shoal barrier is visible in the western tower, as well as the underlying part of the Borca member. B) clinoforms are most evident in the wall in front of the hut. Pay attention to some fallen blocks of layered dolostone, which tilting mimics the dip of clinoforms. C) Deep incisions allow bed-by-bed measurement of the whole Heiligkreuz and Travenanzes formations.

Two main facies associations are exposed here (Figs. 14, 15): a mainly carbonate unit below (facies association A), and a mixed carbonate-siliciclastic unit above (facies association B). Both include mass-

flow deposits and belong to a middle ramp environment.

Facies association A constitutes a ca. 10 m thick succession of mainly oolitic-bioclastic wackestones to grainstones with dm-thick bedding that appear slightly nodular because of bioturbation. Most common fossils are echinoderms, bivalves, and gastropods. Oncoid floatstones are also present, associated with oolitic cross-bedded grainstones. Thin marly interlayers may contain cm- to dm-scale wood fragments.

Intercalated in these well stratified limestones is a wedge of bioclastic packstone with a sharp erosive base cutting 1.5 m into underlying beds, bearing wood fragments and marine fossils such as echinoderms and mollusks.

Finally, a metre-scale patch reef with corals and calcareous sponges in life position (Fig. 16) embedded in rudstones with coral debris can be observed (Fig. 16).

Facies association B is represented by a 5 m thick sequence of metre-scale beds with highly erosive base composed of a mixed carbonate-siliciclastic conglomeratic arenite. Siliciclastic grains are mainly volcanic rock fragments and quartz, and the fossil content is a mixture of continental and marine remains such as plant debris, rare amber droplets, mollusks and echinoderms.

The succession is interpreted as the seaward front of an oolitic-bioclastic shoal barrier. Most of the sedimentary supply is provided by mass flows, either from collapse of the high-relief slope of the shoal behind, or due to river floods triggering hyperpycnal flows. Crossing throughout a carbonate lagoon and shoal, floods may have collected carbonate grains accounting for the mixed carbonate-siliciclastic composition of the succession and for the mixed continental and marine fossil assemblage.

5. The upper Borca member and Dibona Sandstones member

The succession immediately above the dolomitized shoal barrier is exposed along trail n° 421, separated from the outcrop of the previous stop by two faults (Fig. 17).

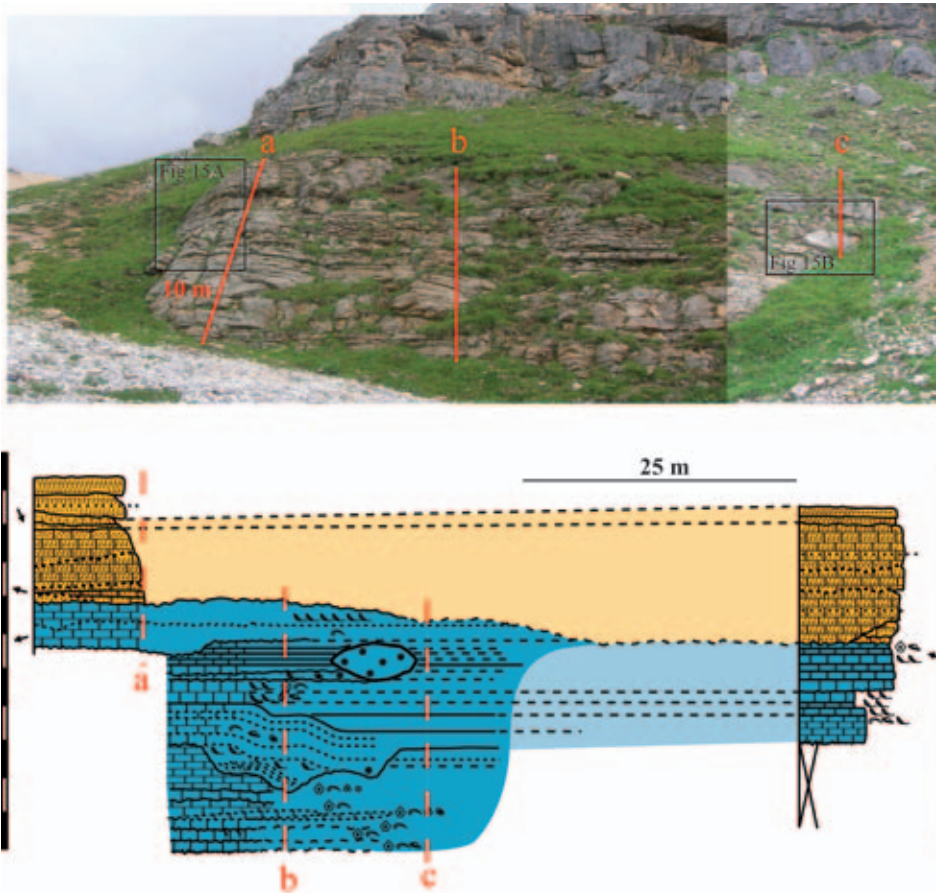


Fig. 14: Outcrop views of stop 4: middle Borca member (picture taken from south to north). Light blue: facies association A (inner-mid ramp); yellow: facies association B (mass flows). Scale bars = 1 m, distances between sections not to scale. Legend in Figure 12.

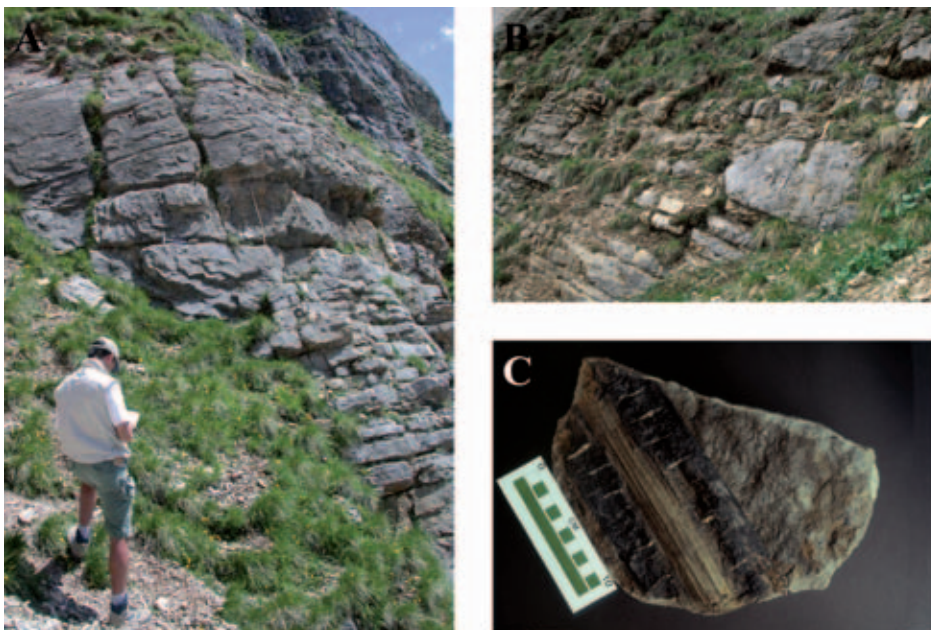


Fig. 15: Outcrop views of stop 4. A) Erosive contact between facies associations A and B. B) the small patch reef embedded in the upper part of facies association A. C) Fragment of Equisetales from the lower-middle Borca member (this specimen is not from this outcrop).

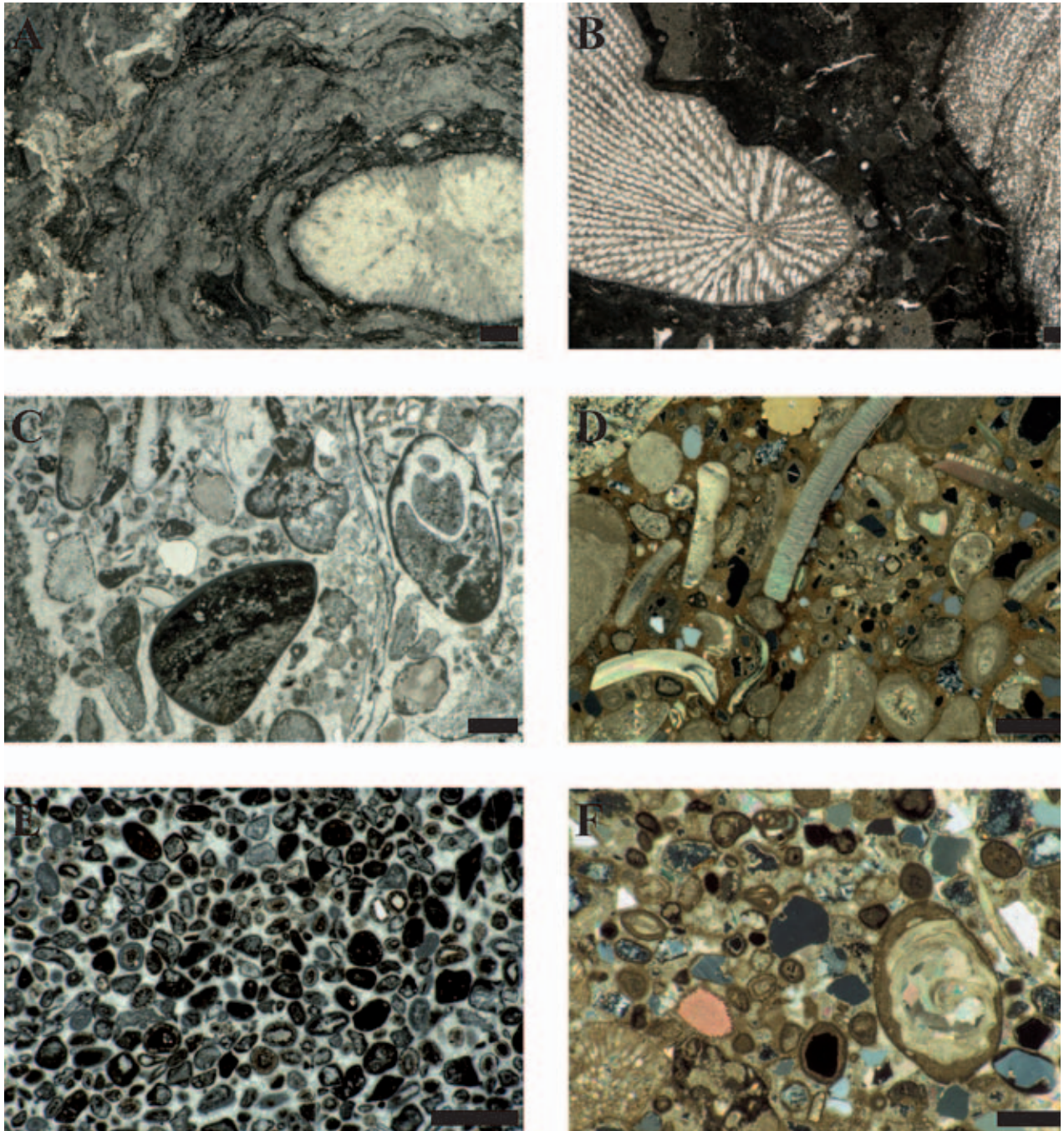


Fig. 16: Microfacies of the lower-middle Borca member. Scale bars = 1mm. A) Coral boundstone with abundant microbial coatings, from the patch reef of stop 4. B) Boundstone with corals and hydrozoans, micritic coatings and automicrite. C) Rudstone with large bioclasts and lithoclasts, deposited laterally to the patch reef of stop 4. D) Grainstone-rudstone with various bioclasts, ooids, oncoids, and sparse siliciclastic grains. E) Oolitic grainstone, a few oolites show siliciclastic nuclei. F) Mixed carbonate siliciclastic arenite with abundant coated grains, belonging to facies association B. Samples of the left column come from stop 4, those of the right column from nearby outcrops with better preservation.

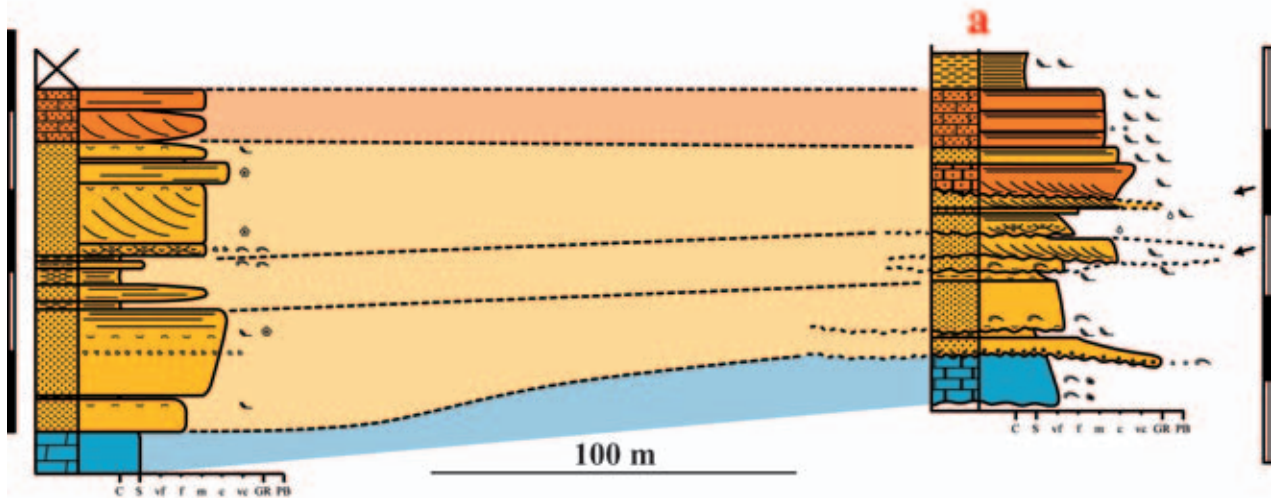


Fig. 17: Outcrop views of stop 5: Upper Borca member (picture taken from east to west). Light blue: lagoon; yellow: shoreface; orange: inner ramp. Scale bars = 1 m. Legend in Figure 12.

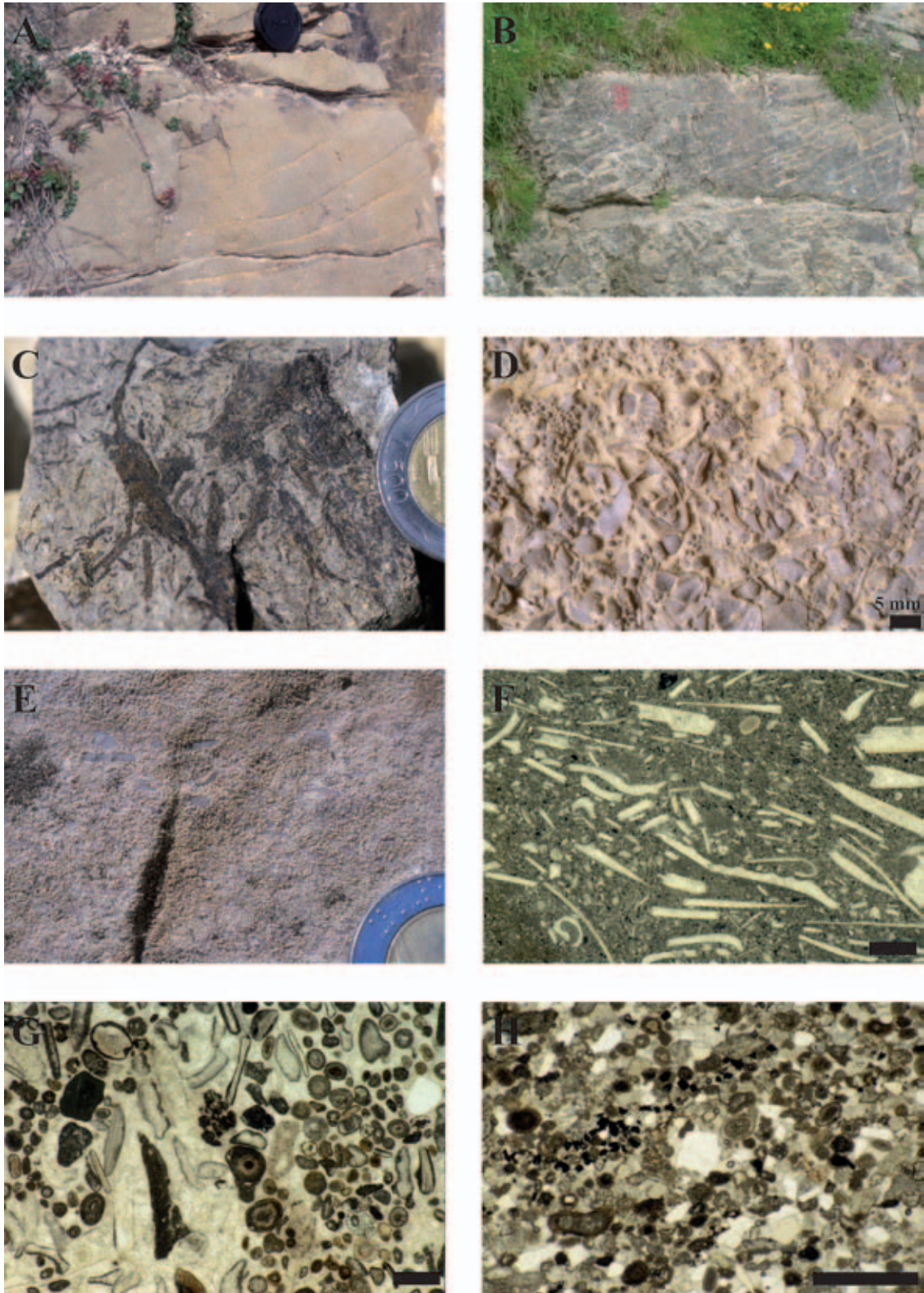


Fig. 18: Facies and microfacies of the upper Borca and Dibona Sandstones members. Scale bars for microfacies = 1 mm, coin = 16 mm. A) dm-scale tangential cross-bedding in oolitic-bioclastic calcarenites of facies association E; B) planar cross-bedding; C) roots in silty marls of facies association E; D) oolitic-bioclastic grainstone (facies association E), with bivalves, gastropods, ostracods, brachiopods, echinoderms; E) flat pebbles in oolitic grainstone (facies association E); F) packstone with fractured bivalve shells (facies association E); G) oolitic-bioclastic grainstone (cf. D); H) hybrid arenite of facies association E.



Fig. 19: Sharp contact between the massive dolomites of the Lagazuoi member and the thin alternation of dark clays and white dolostones of the Travenanzes Fm. The contact is marked by an erosive surface of regional extent.

It is composed of a lower, low energy, mixed carbonate-siliciclastic unit with well developed paleosols (facies association D) followed by an upper, high energy, carbonate-siliciclastic succession without evidence of subaerial exposure (facies association E).

Facies association D is interpreted as a lagoonal succession strongly influenced by terrigenous influx, its seaward embankment being provided by the clinostratified shoal barrier that can be observed in the section immediately below. It is a stack of peritidal sedimentary cycles (Figs. 17, 18), each normally starting with a histic paleosol constituted by dark shales rich in organic matter (see Paleosol box). The cycle may continue with marly limestones and clays with roots, plant debris and amber, and ends with shallow-water carbonates like oolitic-bioclastic packstones-grainstones often capped by supratidal laminites. A paleokarst surface is found at the top of the cycles that cuts into the underlying subtidal carbonate facies. Karstic dissolution and paleosols are best developed at the top of this lithofacies association (Preto and Hinnov, 2003).

Facies Association E consists of arenites, shales, oolitic-bioclastic grainstones with cross bedding in dm-thick layers, and packstone-grainstone layers with normal grading and abundant bivalves usually highly fractured and imbricated (Fig. 18). Trough cross-bedding as well as planar lamination are present. The most

common fossils are mollusks (mainly bivalves) and echi-noderms, but brachiopods, nautiloids, and fragments of marine and terrestrial vertebrate bones and teeth are also present (Preto and Hinnov, 2003). This facies association is mainly terrigenous. It is constituted by fine- to medium-grained arenites with coarser bioclastic lenses and planar cross-bedding, in m-thick layers presenting basal conglomerate lags, rip-up clasts, planar and trough cross-bedding. This facies association was deposited on a shoreface to inner-middle carbonate ramp environment.

6. The Travenanzes Formation: overview

The succession immediately above the Lagazuoi member is well exposed along a rather dangerous gully, upstream with respect to the previous stop, but its architecture is visible from the distance (from the meadow along trail n° 420, at 2198 m asl).

The Travenanzes Fm. is stratigraphically interposed between the Heiligkreuz Fm. (lower Carnian) below and the Dolomia Principale (Norian-Rhaetian) above (Figs. 2, 4, 5).

The lower boundary is sharp and marked by an erosive surface of regional extent. The Travenanzes Fm. rests with an erosive contact on the massive dolomites of the Lagazuoi Member (Fig. 19).

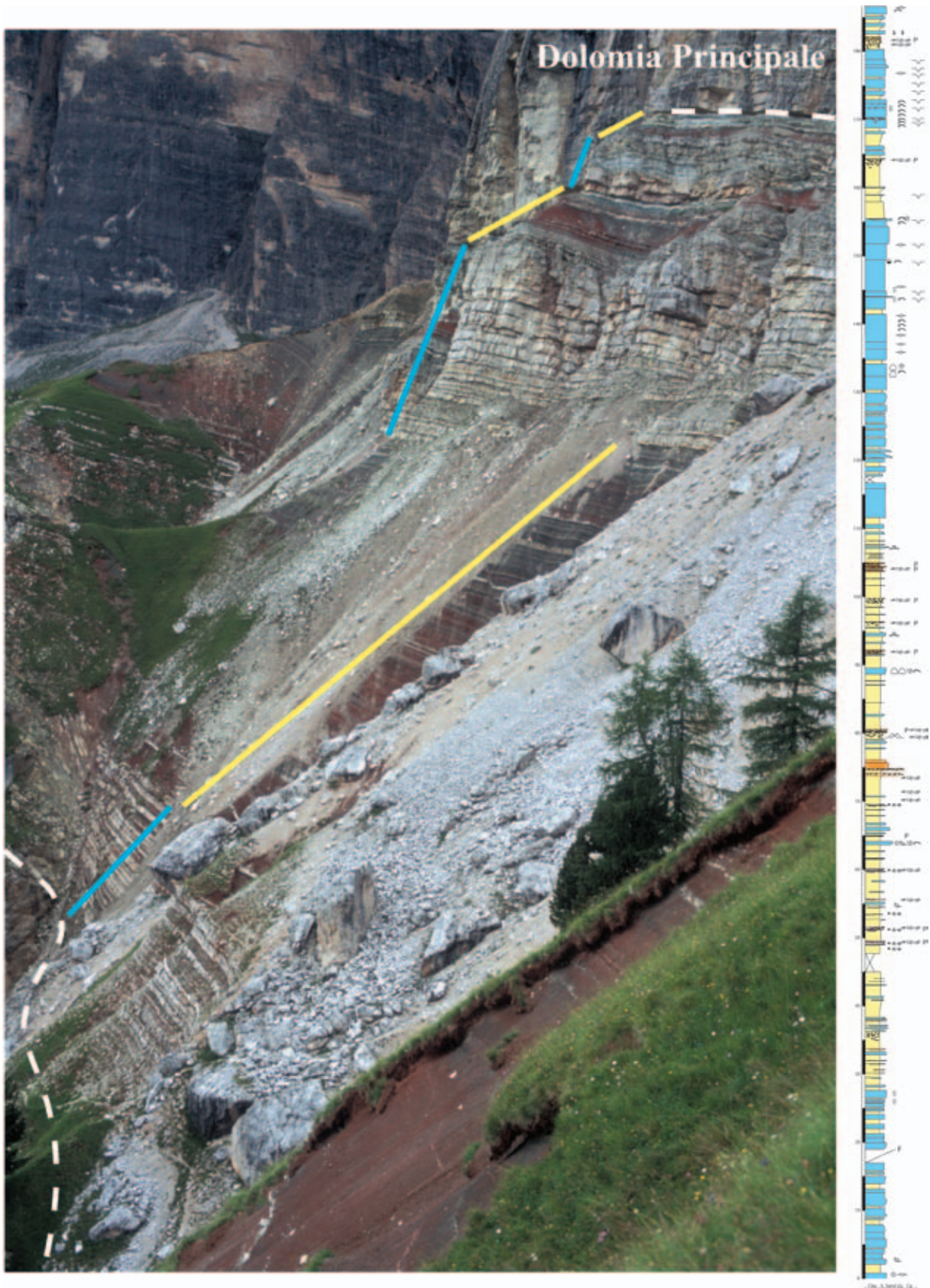


Fig. 20: A) Panoramic view and B) stratigraphic log of the Travenanzes Fm. as seen from 2198 m asl east of the section. Note the three carbonate/siliciclastic sequences and the upward tailing off of the siliciclastic intervals.

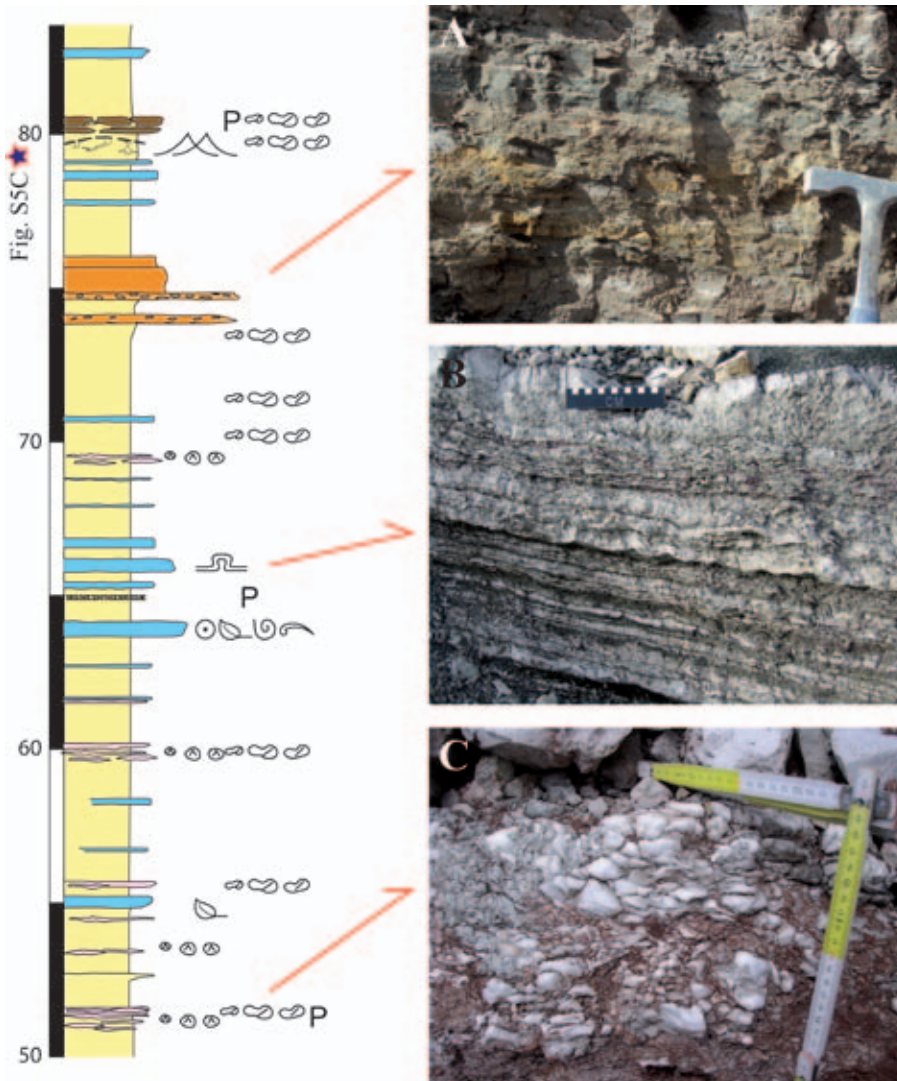


Fig. 21: Stratigraphic log illustrating the flood-basin deposition in the lower siliciclastic interval. Light blue: marine carbonates; pink: evaporites; yellow: mudstones; orange: arenites and conglomerates. Scale bars = 1 m. A) tabular sheet-flood quartz-arenites; B) crinkly algal lamination on top of a carbonate marine storm layer; C) nodular/chicken-wire anhydrite encased in red mudstones.

The upper boundary is gradual and time-transgressive due to a constant decrease of the terrigenous input, and only the complete disappearance of the fine-clastic layers may be used to define the boundary between the two formations.

Three carbonate-siliciclastic cycles are observable (Fig. 20), corresponding to three transgressive-regressive sequences (Breda et al., 2006) and organized in an overall transgressive pattern. A tailing off of the clastic intervals is observed upwards, up to their complete disappearance at the onset of the Dolomia Principale.

Siliciclastic intervals (flood-basin mudstones)

The regressive siliciclastic intervals are mainly made up of multicoloured flood-basin mudstones (Fig. 21). The flood basin is a low-lying coastal mud-flat at the transition between terrestrial and marine deposition. Mudstones were deposited as suspension

load during the temporary inundation of the (otherwise emerged) flood basin, both by sea water during storm surges and by major river floods. Scattered shallow ephemeral stream conglomerates and sheet-flood quartz-arenites, are interpreted as the more distal tails of a terminal-fan fluvial system (Fig. 21A). Few decimeter thick tabular dolomitic layers characterized by a rich marine fauna (bivalves and gastropods) or flat pebble breccias (on top of convoluted algal laminations) are interpreted as tempestites (Fig. 21B). Due to the dominantly arid climate a coastal sabkha developed locally, characterized by nodular/chicken-wire anhydrite encased in red mudstones and organized in saline soil profiles (gypcretes) (Fig. 21C).

Evaporites and calcic paleosols are usually located on top of the regressive interval, the better developed paleosols marking the top of higher-order sequences.

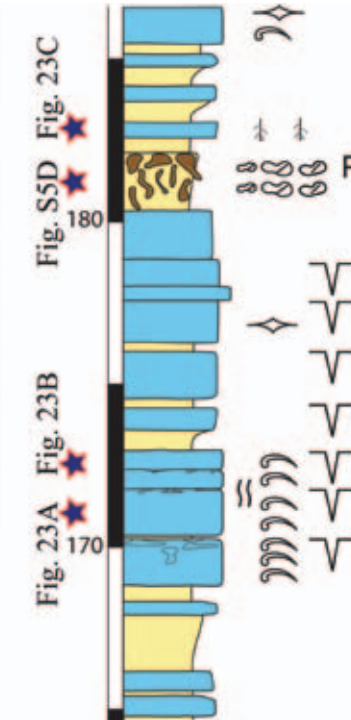
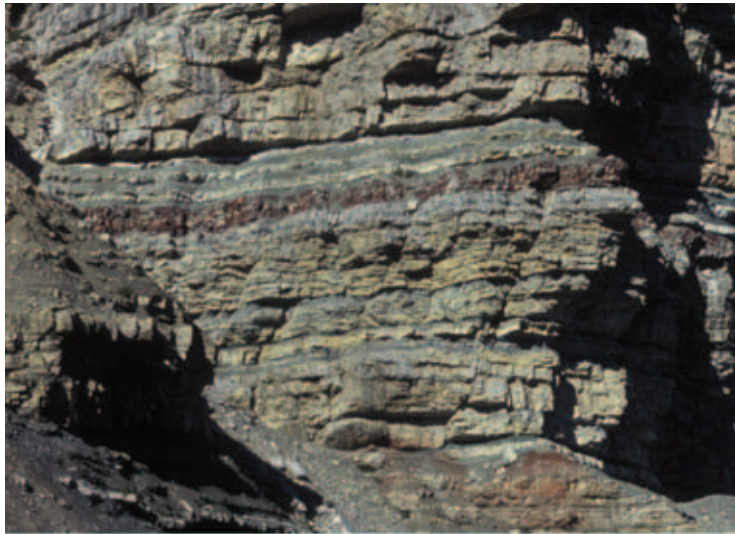


Fig. 22: Panoramic view and stratigraphic log of the upper carbonate/siliciclastic sequence of the Travenanzes Fm. as seen from 2214 m asl west of the section. The carbonate interval is mainly made up of aphanitic, crystalline, algal-laminated and marly dolostones, with subordinate intercalations of prevalently dark mudstones and shales. Note the reddish vertisol at the base of the siliciclastic interval.

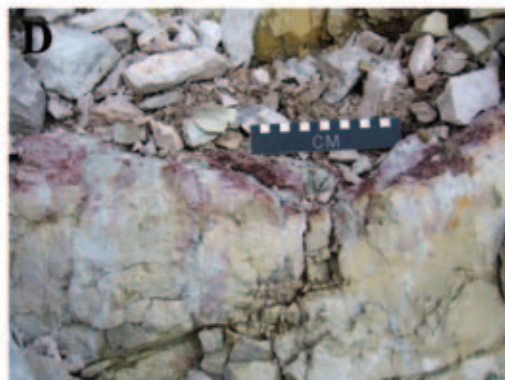
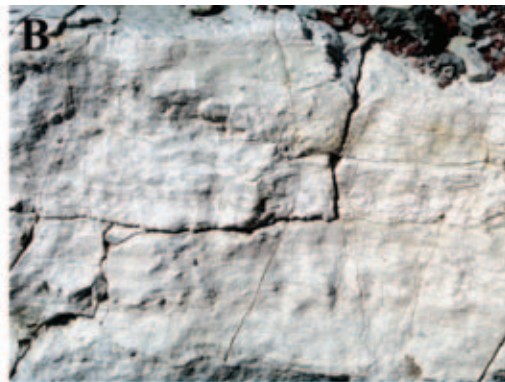
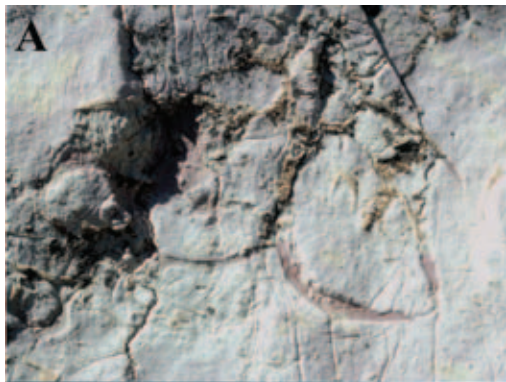


Fig. 23: A) Granular dolostones consisting in wackestone-packstones rich in bivalves (*Megalodontida*). Note the reddish marls infilling the lower part of the bivalve, suggesting dissolution and cementation processes typical of the meteoric diagenesis; B) Irregular dissolution features cut a laminated dolomitic bed characterized by local stromatolites and flat pebble breccias, and are infilled by green dolomitic marls. C) Root traces emanating from a light-grey to whitish dolomite layer: vertical, nearly cylindrical, tubes usually hollow with coarse calcite coatings. D) Root traces emanating from a reddish marly pedoturbated surface: The original organic matter is completely replaced, and only a greenish halo is visible (see Figure 22 for location).

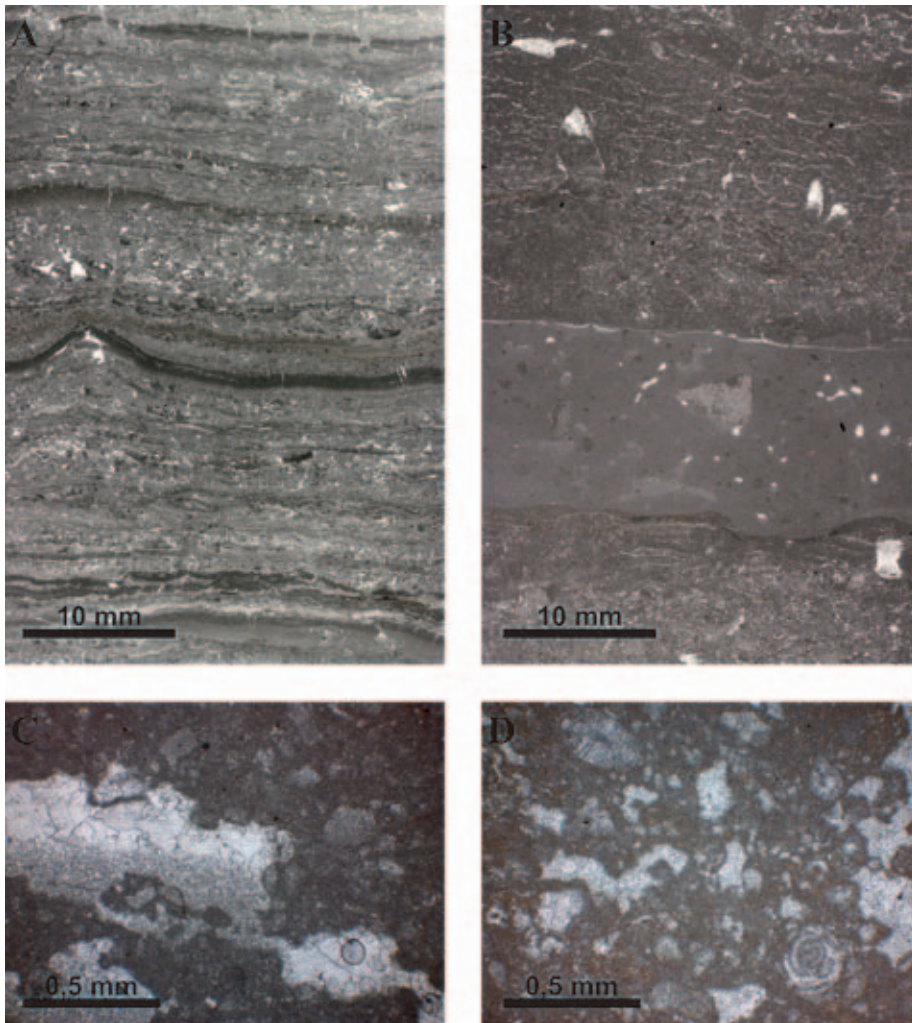


Fig. 24: Microfacies from the upper sequence of the Travenanzes Fm. A) Supratidal algal lamination with micro-tepee and mud crack structures; B) Multilayered sample presenting a lower bed of packstone-grainstones with foraminifera, followed by a massive dolomicrite bed with local intraclasts (interpreted as tempestite), followed in turn by a packstone-wackestone with planar fenestrae; C) Peloidal wackestone with planar fenestrae infilled by geopetal structures with dolomicrite occupying the lower part of the cavity, and sparite cement occupying the space above; D) Bioclastic wackestones rich in foraminifera and diffuse bioturbation.

7. The upper part of the Travenanzes Formation

Following the trail n° 420, the "via ferrata Cengia Astaldi" allows a close determination of the upper part of the Travenanzes Fm., where the carbonate peritidal facies prevails, up to the contact with the Dolomia Principale.

Carbonate intervals (carbonate tidal flat)

The (transgressive) carbonate intervals are characterized by tidal-flat and shallow-lagoon deposition (Figs. 22, 23). Aphanitic, crystalline, algal-laminated and marly dolostones, with subordinate intercalations of prevalently dark mudstones and shales are observed. Aphanitic dolostones consist of light-gray to whitish dolomicrites (mudstones-wackestones) with sparse micritic peloids. Granular dolostones consist of wackestone-packstones to grainstones rich in bivalves (*Megalodontida*) (Fig. 23A), foraminifers and diffuse bioturbation. Peritidal dolostones are

characterized by meter-scale shallowing-upward cycles composed of bioclastic-intraclastic packstones-grainstones rich in bivalves and gastropods. These grade upwards into homogeneous and laminated dolomicrites with local stromatolites and planar fenestrae, and are capped by flat pebble breccias, mud cracks and tepee horizons. The peritidal dolostones are analogous to those characterizing the overlying Dolomia Principale (Figs. 23B, 24).

The thicker crystalline packstone/grainstone beds, rich in marine macrofauna (bivalves and gastropods), suggest a more open, shallow-lagoon setting as confirmed by the green algae (*Dasycladaceans*) and foraminifers observed in thin section. They are usually located in the upper part of the transgressive interval, and mark surfaces of maximum flooding.

CARNIAN PALEOSOLS AT RIFUGIO DIBONA

One way of understanding the climate evolution recorded in the Rifugio Dibona section is to look at paleosols. Paleosols are soils formed on a landscape of the past (e.g., Kraus, 1999) whose physical and chemical characteristics are determined by a few environmental factors, among which climate plays a primary role (e.g., Retallack, 2001). Thus, paleosol features might be used as in-situ climatic indicators and allow the distinction between climatic and local environmental forcing.

Paleosols of the Heiligkreuz Fm. are concentrated in the upper Borca member. Typical paleosol profiles include Fe-illuviation (spodic) horizons or ironstones below well developed histic horizons and may lie on karstified surfaces. Taken together, these features testify for a tropical humid climate (Köppen's A class) with a short - or without - dry season.

In the Travenanzes Fm. paleosols are abundant and well developed. Typical paleosol profiles show a gradual upward increase in the size and density of carbonate nodules constituting the Ca-illuviation (B) horizons of well-drained alkaline soils (calcisols). Calcic vertisols develop in arid-semiarid climates occurring today in tropical belts outside the reach of the Indian summer monsoon (Köppen's B class).

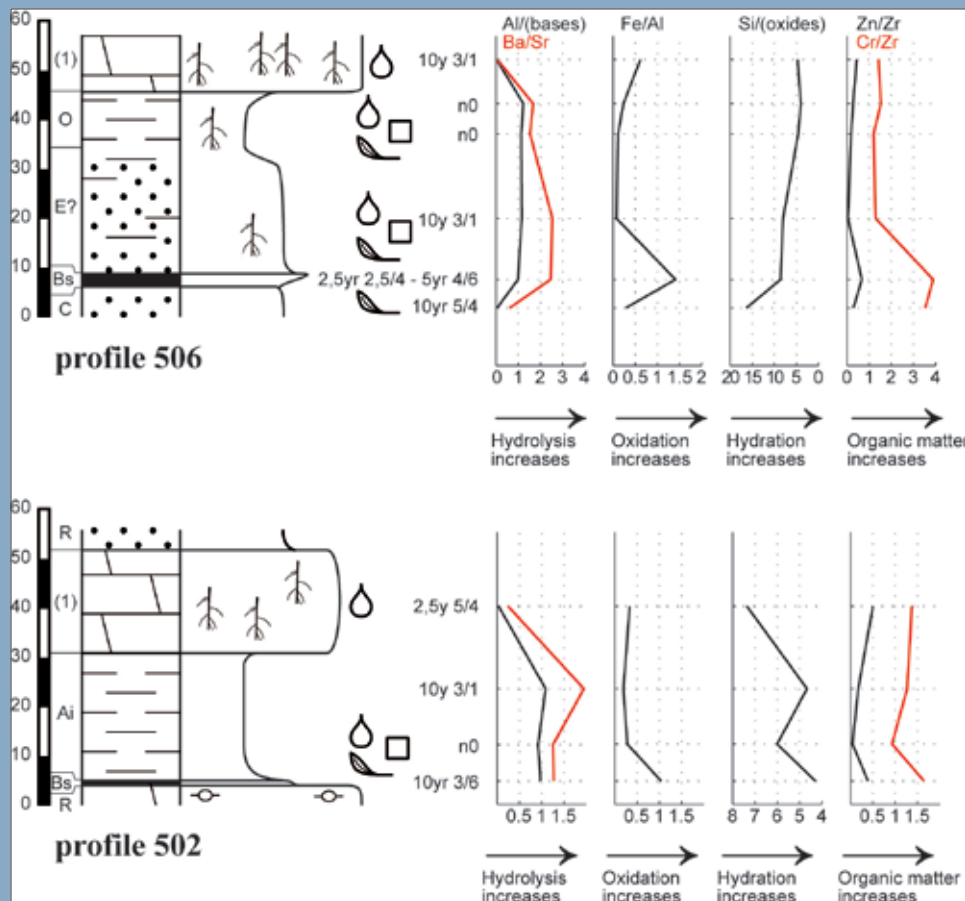


Fig. S1: Paleosols indicative of tropical humid climate of the upper Borca member, Munsell colors of soil horizons, and whole-rock chemical analyses. Suggested soil horizons are indicated to the left; (1) indicates marginal marine sediments related to rapid transgressions. Molecular and atomic ratios indicative of soil processes following Retallack (2001). Scale in cm.



Paleosol 506



Paleosol 502

Fig. S2: Paleosols 506 and 502 are two examples of paleosols with spodic and histic horizons (aquods) lying on siliciclastic and carbonate substratum, respectively.

Climatic indicator	Climatic significance	References
Tepee structures	$E > P$, arid or semiarid tropical climates.	Assereto & Kendall, 1977; Hardie and Shinn, 1986; Mutti, 1994
Evaporites	$E > P$ and commonly $P < 200$ mm.	Retallack, 2001
Calcic horizons and caliches	$E > P$, $P < 760$ mm, arid or semiarid climates.	Royer, 1999; Retallack and Royer, 2000; Retallack, 2001
Karstic dissolution	$P > E$ strongly enhanced by a stable vegetation cover.	Ford and Williams, 1989; Retallack, 2001
Preserved histic horizons	Tropical wet climate with reduced P seasonality, $P \geq 1500$ mm.	Cecil, 1990; Lottes and Ziegler, 1994; Retallack, 2001; cf. Hardie, 1977; Enos and Perkins, 1979
Spodic horizons	$P > E$, wet climate within the tropical belt.	Kraus, 1999; Retallack, 2001

Fig. S3: Primary climatic indicators and their climatic significance. E = mean annual evapotranspiration; P = mean annual precipitation.



Fig. S4: Palaeokarst features. Frequently, irregular dissolution features cut the upper part of the peritidal cycles, infilled by green to reddish dolomitic marls (A) and carbonate micro-breccias (B). Dissolution surfaces in place penetrate vertically as much as 1 m. See also Figure 23A, B.

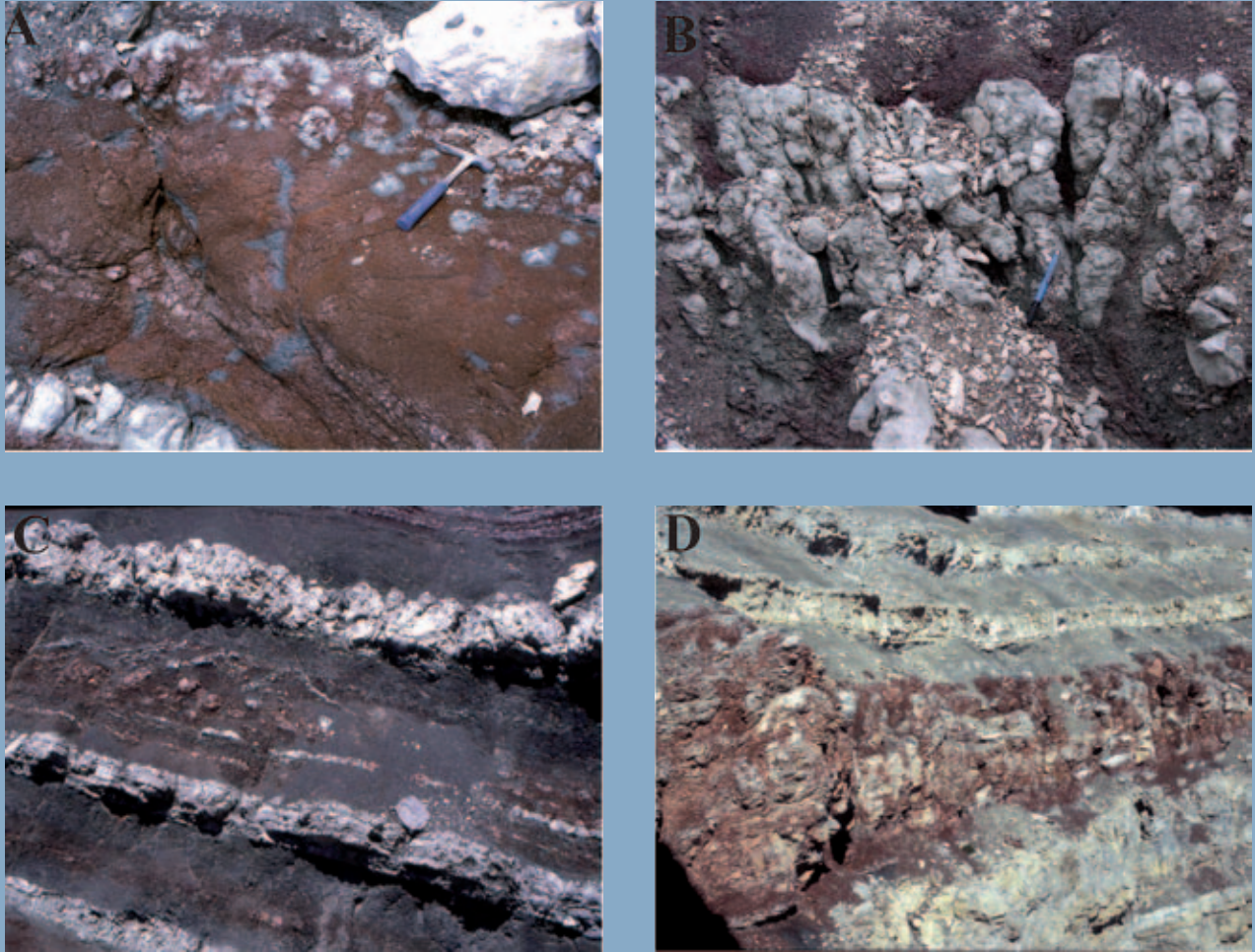


Fig. S5: Calcic and vertic paleosols of the Travenanzes Fm., indicative of semiarid to arid climate, characterized by extreme seasonality. A gradual upward increase in size and density of nodules is commonly observed within paleosol B horizons. A) Carbonate nodules mostly develop in reddish floodplain mudstones. B) Most prominent feature of the vertisols is the vertical elongation of peds, indicating vertical upward and downward movement of water due to alternating wetting and drying conditions. C) Massive hardpan calcrete (caliche) showing a faint prismatic structure with peds separated by narrow, subvertical, mudstone-filled irregular fissures (cutans) extending downwards into the underlying host sediment. Pseudo-anticlinal structures consist of calcite-sealed, slickensided fractures, crossing the mudstone and produced by repeated expansion and contraction of swelling clays. D) Vertisol on top of the Dibona section (see Figure 22 for location).

PALYNOSTRATIGRAPHY OF THE DIBONA SECTION

Palynological analysis of the Heiligkreuz Formation provides information on palynostratigraphy and paleoclimate during the last part of the so called "Carnian Pluvial Event". The generic palynological association found in this formation (Fig. P1, Plate P1) come from the Dibona Sandstones member. The association found in the Travenanzes Formation (Fig. P2, Plate P2) comes from the lowermost levels of this formation, few meters above the Lagazuoi member. The associations found show typical Upper Triassic elements, and particularly association found in the Heiligkreuz Fm. is well comparable with the *Duplicisporites continuus* assemblage whereas the assemblage found at the base of the Travenanzes Fm. is comparable with the *Granuloperculatipollis rudis* assemblage (Roghi, 2004). Both these associations fall into the Densus-Maljawkinae phase of Brugman, 1983 and Van der Eem, 1984.

In the Dibona section, the palynoflora of the upper part of the Heiligkreuz Fm. is characterized by trilete levigate and ornamentated spores, monosaccites and bisaccates pollens and Circumpolles. A quantitative analysis of these levels indicates predominance of conifers (51 %), Pteridosperms (18 %) and Lycopsids, Filicopsida and Sphenopsida (18 %) (Fig. P3, sample DB A). The high percentage of Pteridosperms and Conifers is also indicated in the paleosols by the presence of well preserved cuticule belonging to these groups (Fig. P4) and also for the abundant presence of the fossil resin (see Amber box).

In the lower part of the Travenanzes Fm. (Fig. P3, sample RB 52) the association is characterized by high percentages of Circumpolles (43%), with *Camerosporites secatus* alone constituting 31%; *Ovalipollis* spp. (11%), Lycopsids, Filicopsida and Sphenopsida (16%) and Cycadopites (6 %).

Comparative quantitative analyses of these two samples from the Heiligkreuz Fm. (Dibona Sandstones member) and Travenanzes Fm. and the hygrophytic and xerophytic elements in the palynological assemblages (Fig. P3), show a strong increase in abundance of the xerophytic Circumpolles (between 8% to 42%) and a decrease of monosaccites (from 47% to 8%) and bisaccates (from 18% to 3%). Hygrophytic Azonotriletes maintain constant abundance and indicate the local persistence of humid conditions.

The same trend was found in the time equivalent levels of the Cave del Predil area, Julian Alps (De Zanche et al., 2000, Roghi, 2004). Here, from the upper Tor Fm. to the lowermost Carnitza Fm. a decrease of monosaccites and bisaccates is linked with a rapid increase of Circumpolles forms. Their presence could be linked to the final phase of the humid pulse, well testified both in the Dolomites and in the Julian Alps, with a strong increase of the Circumpolles groups in the Travenanzes Fm. and in the Carnitza Fm. respectively.

Species (Heiligkreuz Formation)	Botanical affinity	%
Levigated and ornamentated spores, genus <i>Calamospora</i> , <i>Todisporites</i> , <i>Concavisporites</i> , <i>Retusotriletes</i> and <i>Uvaesporites</i>	Lycopsids, Filicopsida and Sphenopsida	13
<i>Spiritisporites spirabilis</i> Scheuring, 1970	? Filicopsida	< 1
<i>Vallasporites ignacii</i> Leschik in Kräusel and Leschik, 1956	Conifers	8
<i>Enzonalasporites vigens</i> Leschik in Kräusel and Leschik, 1956	Conifers	10
<i>Patinasporites</i> cf. <i>densus</i> (Leschik, 1956) Scheuring, 1970	Conifers	2
<i>Patinasporites densus</i> (Leschik, 1956) Scheuring, 1970	Conifers	1
<i>Pseudoenzonalasporites summus</i> Scheuring, 1970	Conifers	1
<i>Samaropollenites speciosus</i> Goubin, 1965	Conifers or Pteridosperms	1
<i>Ovalipollis pseudoalatus</i> (Thiergart, 1949) Schuurman, 1976	?Cycadales, ?Pteridosperms, ?Conifers	8
<i>Lunatisporites acutus</i> Leschik in Kräusel and Leschik, 1956	Pteridosperms (Peltaspermales), ?Conifers, ?Podocarpaceae	4
<i>Infernopollenites parvus</i> Scheuring, 1970	Pteridosperms (Peltaspermales), ?Conifers	<1
<i>Triadispora</i> spp.	Conifers (Voltziales)	8
<i>Lueckisporites</i> sp.	Conifers (Majonicaceae)	3
alete bisaccate	Pteridosperms (Peltaspermales), Conifers	29
<i>Duplicisporites continuus</i> Praehauser-Enzenberg, 1970	Conifers (Cheirolepidiaceae)	1
<i>Paracirculina maljawkinae</i> Klaus, 1960	Conifers (Cheirolepidiaceae)	3
<i>Duplicisporites verrucosus</i> (Leschik, 1956) Scheuring, 1970	Conifers (Cheirolepidiaceae)	1
<i>Duplicisporites granulatus</i> (Leschik, 1956) Scheuring, 1970	Conifers (Cheirolepidiaceae)	6
<i>Camerosporites secatus</i> Leschik in Kräusel and Leschik, 1956	Conifers (Cheirolepidiaceae), ?Pteridosperms	<1

Fig. P1: Palynological association, botanical affinity and quantitative data from the upper part of the Heiligkreuz Fm. (from Roghi et al., 2006). Percentages are related to a complex of samples collected in the in the Heiligkreuz Fm. (Dibona and Heiligkreuz sections).

Species (Travenanzes Formation)
<i>Concavisporites</i> sp.
<i>Todisporites</i> sp.
<i>Verrucosisporites</i> sp.
<i>Carnisporites ornatus</i> Mädler 1964
<i>Converrucosisporites</i> sp.
<i>Laricoidites intragranulosus</i> Bharadway and Singh, 1964
<i>Aratrisporites</i> sp.
<i>Vallasporites</i> sp.
<i>Vallasporites ignacii</i> Leschik, 1956
<i>Enzonalasporites vigens</i> Leschik, 1956
<i>Ovalipollis</i> spp.
<i>Camerosporites secatus</i> (Leschik, 1956) Scheuring 1978
<i>Granuloperculatipollis</i> sp.
<i>Granuloperculatipollis rudis</i> (Venkatachala and Góczán, 1964)
Mostler et al., 1978
<i>Riccisporites</i> cf. <i>R. tuberculatus</i>

Fig. P2: Palynological association from the lower part of the Travenanzes Fm. in the Dibona section.

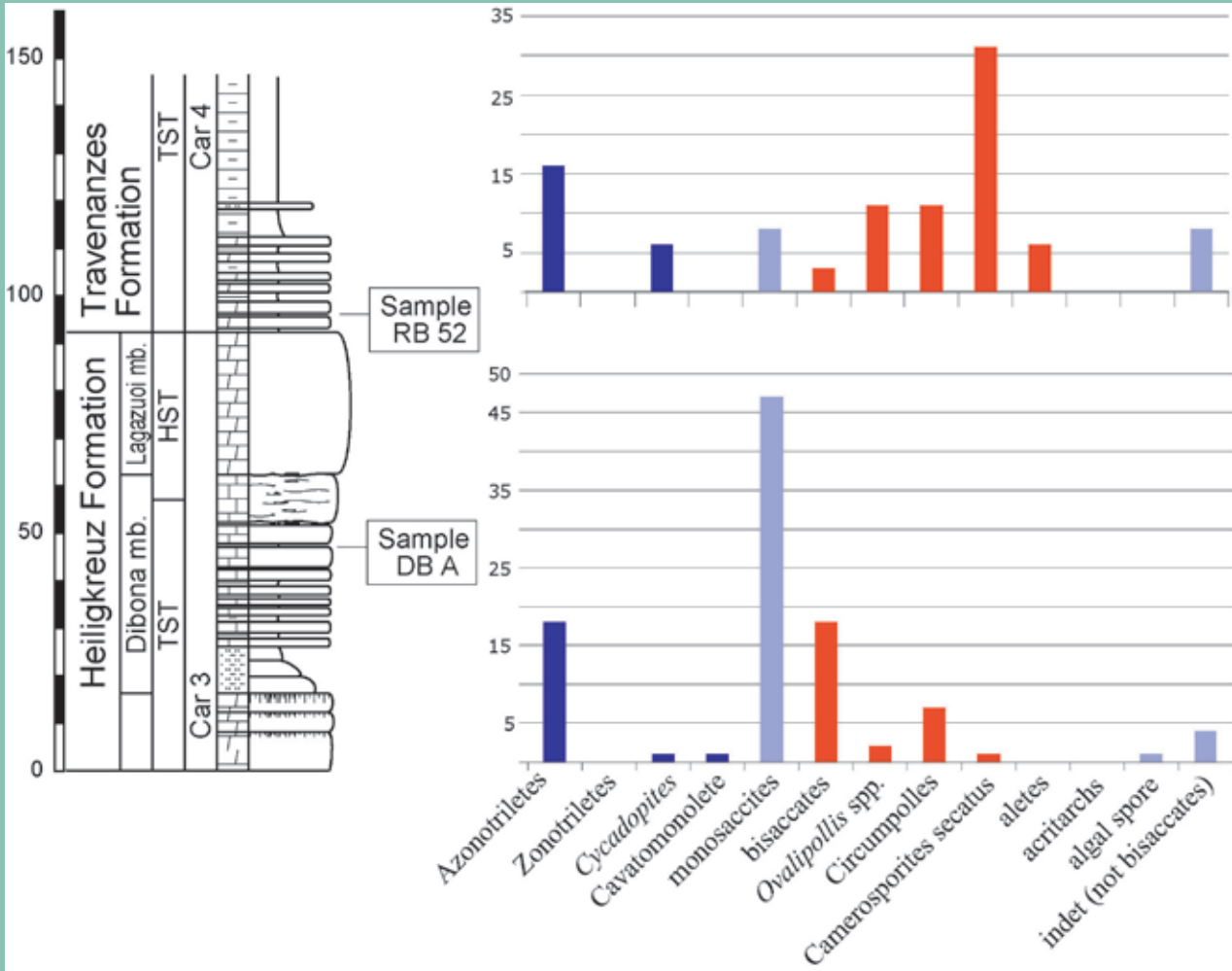


Fig. P3: Quantitative distribution of the main palynomorph groups in the upper part of the Heiligkreuz Fm. (sample DB A) and in the lowermost part of the Travenanzes Fm. (sample RB 52).

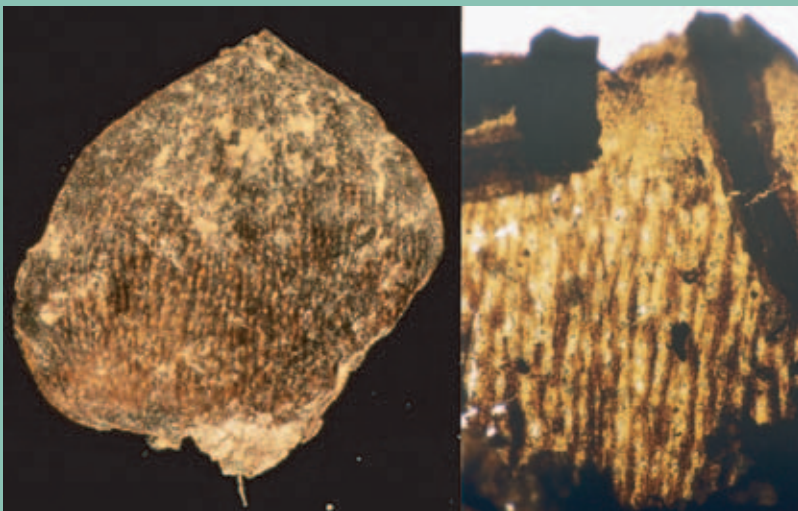


Fig. P4: Fossil leaves with Conifer affinity from the most rich of amber paleosol of the Dibona section (upper part of the Dibona Sandstones member, Heiligkreuz Fm.).

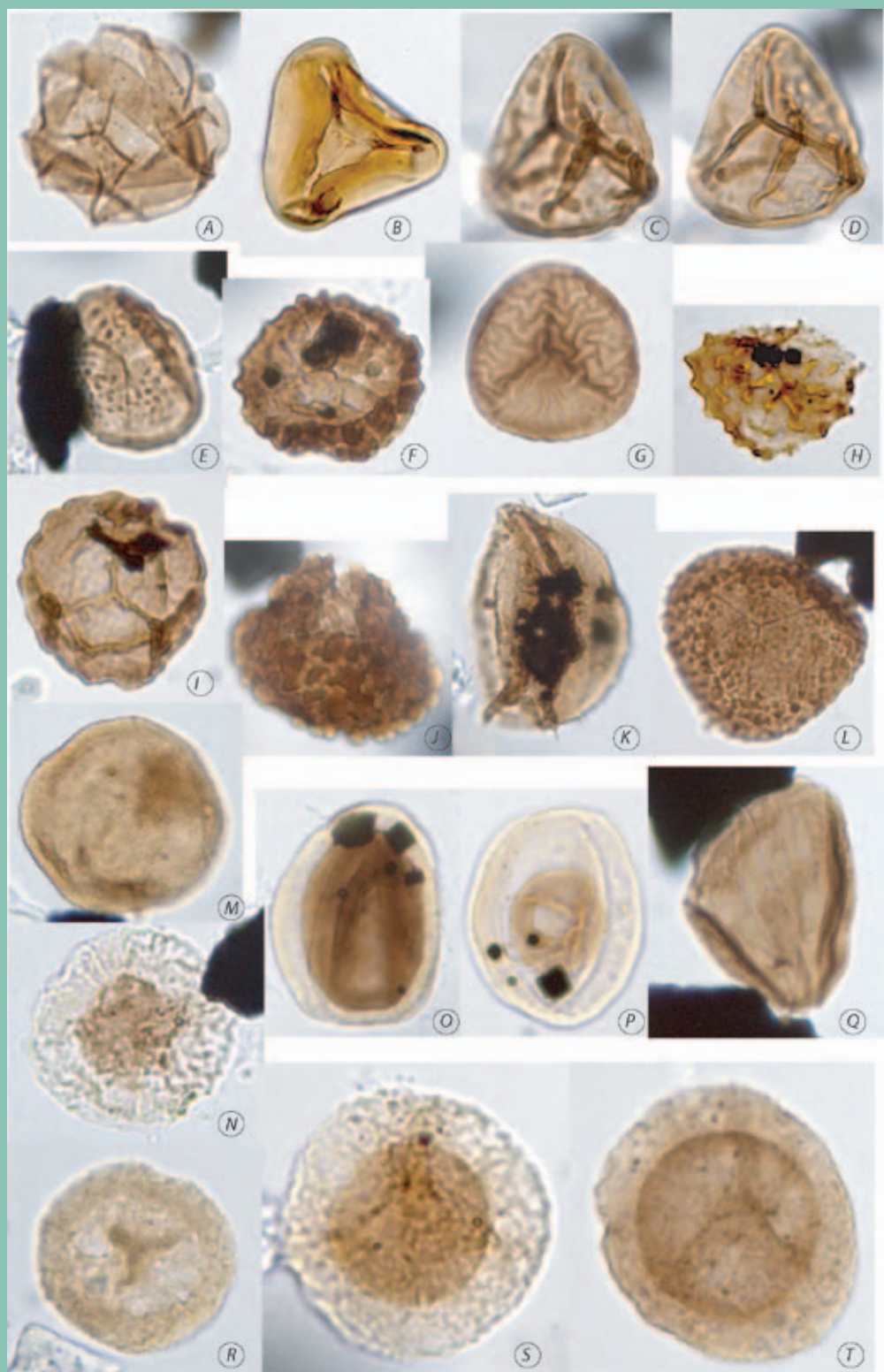


Plate P1 Palynological association from the Heiligkreuz Fm.: A) *Calamospora lunzensis*, (39 μm); B) *Concavisporites* sp., (50 μm); C, D) *Leptolepidites* cf. *L. verrucatus*, (30 μm); E) *Nevesisporites vallatus*, (30 μm); F) *Uvaesporites gadensis*, (25 μm); G) *Lycopodiacidites keupperi*, (37 μm); H) *Gibeosporites hirsutus*, (25 μm); I) *Anapiculatisporites telephorus*, (30 μm); J) *Combaculatisporites mesozoicus*, (38 μm); K) *Aratrisporites parvispinosus*, (41 μm high); L) *Converrucosisporites tumulosus*, (40 μm), M) *Pseudoenzonalasporites summus*, (37 μm); N) *Patinasporites* cf. *P. densus*, (30 μm); O) *Paracirculina maljawkinae*, (30 μm); P) *Duplicisporites continus*, (35 μm); Q) *Equisetosporites chinleanus*, (34 μm high); R) *Vallasporites ignacii*, (30 μm); S, T) *Tulesporites* sp., (S, 42 μm , T, 37 μm).

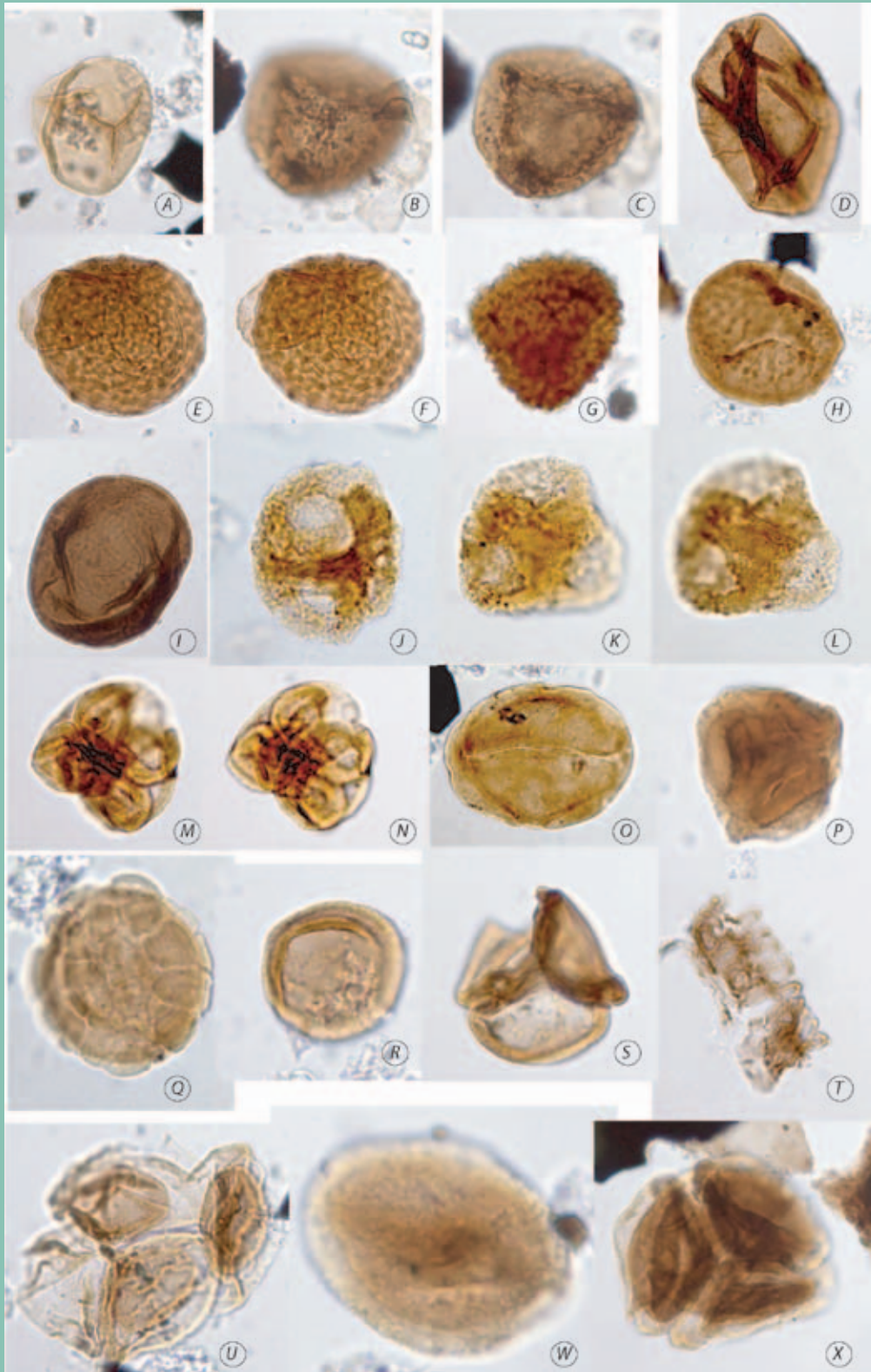


Plate P2 Palyonological association from the Travenanzes Fm.: A) *Todisporites* sp., (46 μ m); B, C) *Convruccosisporites* sp., (50 μ m); D) *Laricoidites intragranulosus*, (56 μ m long); E, F) *Verrucosisporites* sp., (62 μ m); G) *Combaculatisporites* sp., (48 μ m); H) *Carnisporites ornatus*, (36 μ m); I) *Laricoidites intragranulosus*, (56 μ m long); J, K, L) *Vallasporites* sp., (J, 37 μ m, K,L, 32 μ m); M, N) *Riccisporites* cf. *R. tuberculatus*, (35 μ m); O) *Ovalipollis ovalis*, (64 μ m long); P) *Granuloperculatipollis* sp., tetrads, (32 μ m); Q) *Camerosporites secatus*, (31 μ m); R) *Granuloperculatipollis* sp., (27 μ m); S) *Riccisporites* cf. *R. tuberculatus*, (27 μ m); T) spirally plant fragments, (20 μ m large); U) cavate forms, tetrads, (40 μ m); W) *Aratrisporites* sp., (32 μ m); X) *Granuloperculatipollis rudis*, (40 μ m).

THE TRIASSIC AMBER OF THE DOLOMITES

Upper Triassic strata of the Heiligkreuz Formation preserve, like a precious treasure, the most ancient and quantitatively substantial amber deposits of the world (Fig. A1). Amber is fossilized resin of ancient trees that grew in the near land. Amber of the Heiligkreuz Fm. was found in (i) hybrid sandstone, with marine pelecypods and plant debris suggesting that the amber was transported and redeposited, and (ii) in palaeosols associated with plant remains indicating an autochthonous origin. In the palaeosol a considerable abundance of cuticle-preserved leaves allowed the correlation of the amber-producing species to the family Cheirolepidiaceae, a group of conifers present in the near land, as indicated also by palynological analysis (Roghi et al., 2006b). The fossil resin drops found in the palaeosol show typical globe-shaped forms with a little stem and a main diameter of 2-3 mm; some of the outer drop surfaces show characteristic reticular structures suggesting a fast desiccation (Fig. A1).

This fossil resin was first reported by Koken (1913) in his famous posthumous work on the mollusk and vertebrate fauna of Heiligkreuz. Later it was described by Zardini (1973) and Wendt & Fürsich (1980), but only recently this amber was extensively studied not only with respect to its physico-chemical properties, but also with the purpose to understand its palaeobotanical origin (Gianolla et al., 1998b; Roghi et al., 2006a, 2006b; Ragazzi et al., 2003).

Triassic amber of the Dolomites comes only from the Heiligkreuz Fm., corresponding to a time interval between Early and Late Carnian. In the same chronostratigraphic interval fossil resin was found also in a wide area including the Schilfsandstein (Switzerland), the Raiblerschichten and Lunzerschichten (Austria), the Barnag member of the Sándorhegy Formation (Hungary) and the Chinle Formation (Arizona) (Fig. A2 and references therein). These defined and restricted findings could suggest that resin exudation from the ancient trees could have been influenced by some kind of palaeopathology probably caused by palaeoclimatic fluctuations.

The identity card for the Triassic amber of Dolomites was obtained through many physico-chemical studies (Ragazzi et al., 2003; Roghi et al., 2006b). Main analyses were infrared spectrophotometry (FTIR), nuclear magnetic resonance (NMR), thermogravimetry (TG), differential thermogravimetry (DTG), and automated elemental analysis. The infrared spectrum of the Triassic amber is typical of fossil resins (Fig. A3) but presents a peculiar shape of the fingerprint region.

When inside this amber a rich microbiological world was discovered (Fig. A4), a more complete investigation of these microorganisms started in collaboration with Dr. Alexander Schmidt (University of Berlin) and Prof. Olimpia Coppellotti (University of Padova) (Schmidt et al., 2006). The study on fossil microorganisms embedded in the amber, still preserved at an astonishingly pristine state, is still in progress. The overall of these data suggests that Triassic amber of the Dolomites is a unique kind of fossil resin with interesting potentials also as a palaeoenvironmental indicator.



Fig. A1: Amber drops found in the palaeosols in the Heiligkreuz Fm., Dolomites.

Age		DOLOMITES (Italy) (Koken, 1913; Gianolla et al., 1998; Roghi et al., 2006b)	BALATON HIGHLAND (Hungary) (Budai et al., 1999; Gábor and Földvári, 2005)	Eastern NCA (Lunz area) (Austria) (Sigmund 1937 in Vávra, 1984)	Western NCA (Kochental, Tyrol) (Pichler, 1868)	NEUEWELT (Switzerland) (Soom, 1984, Kelber and Hansch, 1996)	NE ARIZONA (USA) (Litwin and Ash, 1991)
C A R N I A N	J U L I A N	RAIBL FM.		OPPONITZER-SCHICHTEN	RAIBLERSCHICHTEN ("TORER SCHICHTEN") shales 2b-2c	UNTERE KIESELSANDSTEIN	PAINTED DESERT MB. SONSELA MB.
		HEILIGKREUZ SANTA CROCE Fm.	SANDORHEGY FM.	LUNZER-SCHICHTEN RAINGRABENER SCHICHTEN	RAIBLERSCHICHTEN ("CARDITA SCHICHTEN") shales 1a-1b-1c-2a	ROTE WAND HAUPTSTEIN-MERGEL SCHILFSANDSTEIN	BLUE MESA MB. MESA REDONDO FM. SHINARUMP FM.
		S. CASSIANO FM.	VESZPREM FM.	GOSTLINGER KALK	WETTERSTEINKALK	GIPSKEUPEK	

ammonoids
 palynomorphs
 hiatus
 amber

Fig. A2: Localities of Upper Triassic fossil resin.

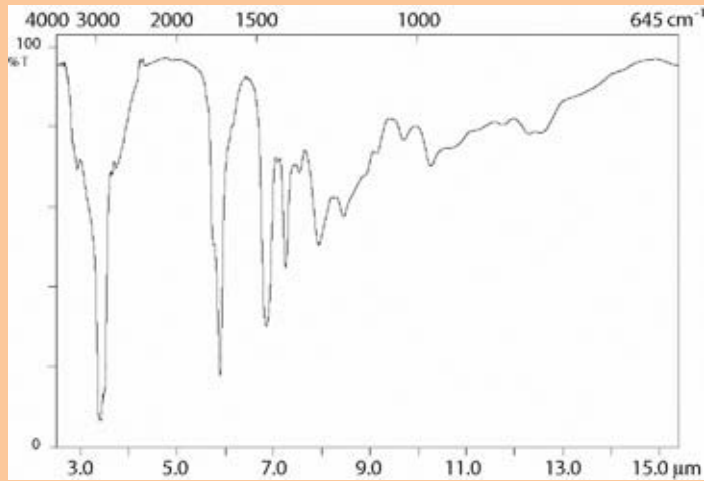


Fig. A3: Solid-state FTIR spectrum of Triassic amber from the Dolomites (from Roghi et al., 2006b).

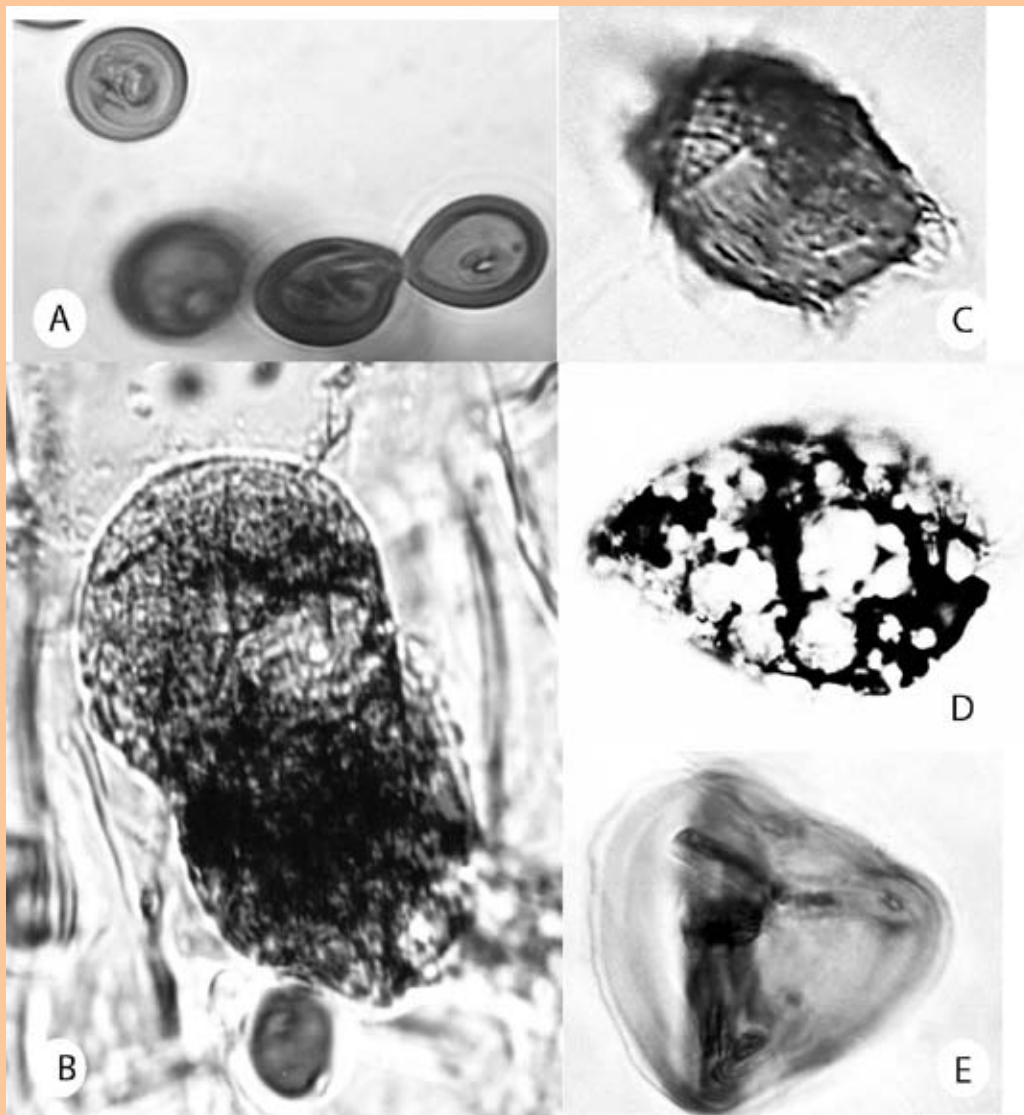


Fig. A4: Microinclusion in the Triassic amber from the Dolomites (from Schmidt et al., 2006). A) Chrysophycean cysts, diameter 10–20 μm ; B) Conifer pollen, 120 μm length; C) Coleps, Ciliate inclusion; D) Cyst of rhizopod protozoan, diameter 20 μm ; E) fern spore, 40 μm in diameter.

Dedication

We dedicate this work to the memory of the late Vittorio De Zanche, our mentor and friend.

Photograph (August 21, 1997): Vittorio during fieldwork in the Rifugio San Marco section at Heiligkreuz (San Vito di Cadore).



References

- Assereto, R. & Kendall, C.G..St.C. (1977): Nature, origin and classification of peritidal tepee structures and related breccias. – *Sedimentology*, 24: 153–210.
- Avanzini, M., Dalla Vecchia, F.M., De Zanche, V., Gianolla, P., Mietto, P., Preto, N. and Roghi, G. (2000): Aspetti stratigrafici relativi alla presenza di tetrapodi nelle piattaforme carbonatiche mesozoiche del Sudalpino. – *Acc. Naz. Sc., Let. Arti Modena, Collana di Studi*, 21: 15–20.
- Baccelle Scudeler, L. & Grandesso, M. (1989): Pisoidi della Dolomia di Durrenstein (Carnico superiore) in Valparola – Dolomiti centrali (Italia settentrionale). – *Mem. Sci. Geol.*, 41: 37–49.
- Bosellini, A. (1984): Progradation geometries of carbonate platforms: examples from the Triassic of the Dolomites, Northern Italy. – *Sedimentology*, 31: 1–24.
- Bosellini, A. (1967): La tematica deposizionale della Dolomia Principale (Dolomiti e Prealpi Venete). – *Boll. Soc. Geol. It.*, 86: 133–169.
- Bosellini, A. & Hardie, L.A. (1988): Facies e cicli della Dolomia Principale delle Alpi Venete. – *Mem. Soc. Geol. It.*, 30: 245–266.
- Bosellini, A., Dal Cin, R. and Gradenigo, A. (1978): Depositi litorali raibliani nella zona di Passo Falzarego (Dolomiti centrali). – *Ann. Univ. Ferrara (N.S.)*, sez. IX, vol.V, 13: 223–238.
- Bosellini, A., Masetti, D. and Neri, C. (1982): La geologia del passo del Falzarego. In *Guida alla Geologia del Sudalpino centro-orientale* (Castellarin A., Vai G. B. eds.). – *Guide geologiche regionali della Soc. Geol. It.*: 273–278.
- Bosellini, A., Neri, C. and Stefani, M. (1996): *Geologia delle Dolomiti, introduzione geologica*. – 78° riunione estiva della Soc. Geol. It.: 9–53.
- Bosellini, A., Gianolla, P. and Stefani, M. (2003): The Triassic carbonate platforms of the Dolomites (northern Italy): their evolution and stratigraphic framework. – *Mem. Sci. Geol.*, 54: 111–114.
- Breda, A., Massari, F., Meneguolo, R. and Preto, N. (2006): An alluvial plain – sabkha – lagoon system in the Upper Triassic of the Dolomites, northern Italy. – *Abstract Book: EGU General Assembly 2006*, Vienna.
- Breda, A. & Preto, N. (2008): A continental/siliciclastic to shallow-marine/carbonate system in the Upper Triassic of Dolomites (Travenanzes Formation, N Italy). – *Rendiconti online Soc. Geol. It.*, 2: 51–56.
- Broglio Loriga, C., Cirilli, S., De Zanche, V., Di Bari, D., Gianolla, P., Laghi, G.F., Lowrie, W., Manfrin, S., Mastandrea, A., Mietto, P., Muttoni, G., Neri, C., Posenato, R., Reichichi, M., Rettori, R. and Roghi, G. (1999): The Prati di Stuoere/Stuore Wiesen Section (Dolomites, Italy): a candidate Global Stratotype Section and Point for the base of the Carnian stage. – *Riv. It. Paleont. Stratigr.*, 105: 37–78.
- Brugman, W.A. (1983): Permian–Triassic palynology. – 122 pp., *Lab. Palaeob. Palynol.*, Univ. Utrecht, Utrecht.
- Budai, T., Császár, G., Csillag, G., Dudko, A., Koloszá, L. and Majoros, G.. (1999): A Balaton-felvidék földtana. – 257 pp., *Geological Institute of Hungary*, Budapest.
- Castellarin, A. & Doglioni, C. (1985) – A geologic schematic cross-section of the Southern Alps. – *Rendiconti Soc. Geol. It.*, 8: 35–36.
- Cecil, C.B. (1990): Paleoclimate controls on stratigraphic repetition of chemical and siliciclastic rocks. – *Geology*, 18: 533–536.
- De Zanche, V., Gianolla, P., Mietto, P., Siorpaes, C. and Vail, P.R. (1993): Triassic sequence stratigraphy in the Dolomites (Italy). – *Mem. Sci. Geol.*, 45: 1–27.
- De Zanche, V., Gianolla, P. and Roghi, G. (2000): Carnian stratigraphy in the Raibl/Cave del Predil area (Julian Alps, Italy). – *Eclogae Geol. Helv.*, 93: 331–347.

- Enos, P. & Perkins, R.D. (1979): Evolution of Florida Bay from island stratigraphy. – *Geol. Soc. Am. Bull.*, 90: 59-83.
- Ford, D. & Williams, P. (1989): Karst geomorphology and hydrology. – Unwin Hyman, London, 601 pp.
- Gábor, C. & Földvári, M. (2005): Upper Triassic amber fragments from the Balaton Highland, Hungary. – *A Magyar Állami Földtani Intézet Évi Jelentése*, 2005, pp. 37-46.
- Gianolla, P., De Zanche, V. and Mietto, P. (1998a): Triassic sequence stratigraphy in the Southern Alps (northern Italy): definition of sequences and basin evolution. – In: de Graciansky, P.-C., Hardenbol, J., Jacquin, T. & Vail, P.R. (eds.), *Mesozoic and Cenozoic sequence stratigraphy of European basins*, SEPM Spec. Publ., 60: 719-747.
- Gianolla, P., Roghi, G. and Ragazzi, E., (1998b): Upper Triassic amber in the Dolomites (Northern Italy). A paleoclimatic indicator? – *Riv. It. Paleont. Stratigr.*, 104: 381-390.
- Gianolla, P., De Zanche, V. and Roghi, G. (2003): An Upper Tuvanian (Triassic) platform-basin system in the Julian Alps: the start-up of the Dolomia Principale (Southern Alps, Italy). – *Facies*, 49: 135-150.
- Gianolla, P., Micheletti, C., Panizza, M. and Viola, F. (2008): Nomination of the Dolomites for Inscription on the World Natural Heritage List Unesco. – *Artimedia*, Trento, 367 pp.
- Hardie, L.A. (1977): Sedimentation on the modern carbonate tidal flats of northwest Andros Island, Bahamas. – *The Johns Hopkins University press*, Baltimore, 202 pp.
- Hardie, L.A. & Shinn, E.A. (1986): Carbonate depositional environments modern and ancient, 3, Tidal flats. – *Quat. Jour. Colorado School Min.*, 81: 1-74.
- Keim, L. & Schlager, W. (2001): Quantitative compositional analyses of a Triassic carbonate platform (Southern Alps, Italy). – *Sediment. Geol.*, 139: 261-283.
- Keim, L., Brandner, R., Krystyn, L. and Mette, W. (2001): Termination of carbonate slope progradation: an example from the Carnian of the Dolomites, Northern Italy. – *Sediment. Geol.*, 143: 303-323.
- Kelber, K.P. & Hansch, W. (1996): Keuperpflanzen Die Enträtselung einer über 200 Millionen Jahre alten Flora. – *Museo*, 11: 1-157, Heillbronn.
- Kelly, S.B. & Olsen, H. (1993): Terminal fans – a review with reference to Devonian examples. – *Sediment. Geol.*, 85: 339-374.
- Koken, E., (1913): Kennntnis der Schichten von Heiligenkreuz (Abteital, Südtirol). – *Abhandlungen der Kaiserlich-Königlichen Geologischen Reichsanstalt*, 16: 1-43.
- Kraus, M.J. (1999): Paleosols in clastic sedimentary rocks: their geologic applications. – *Earth Sci. Rev.*, 47: 41-70.
- Leonardi, P. (1968): Le Dolomiti: geologia dei monti tra Isarco e Piave. – *Manfrini Editore*, Trento, 1019 pp.
- Litwin, R.J. & Ash, S.R. (1991): First early Mesozoic amber in the western hemisphere. – *Geology*, 19: 273-276.
- Lottes, A. & Ziegler, A.M. (1994): World peat occurrence and the seasonality of climate and vegetation. – *Paleogeogr. Paleoclimatol. Paleoecol.*, 106: 23-37.
- Mutti, M. (1994): Association of tepees and paleokarst in the Ladinian Calcare Rosso (Southern Alps, Italy). – *Sedimentology*, 40: 621-641.
- Neri, C. & Stefani, M. (1998): Sintesi cronostratigrafica e sequenziale dell'evoluzione permiana superiore e triassica delle Dolomiti. – *Mem. Soc. Geol. It.*, 53: 417-463.
- Neri, C., Gianolla, P., Furlanis, S., Caputo, R. and Bossellini, A. (2007): Carta Geologica d'Italia alla scala 1:50000, foglio 29 Cortina d'Ampezzo, and Note illustrative. – *APAT*, Roma, 200 pp.
- Pichler, A. (1868): Beiträge zur Geognosie Tirols. XI. – Fossiles Harz. – *Jahrbuch der Kaiserlich-Königlichen Geologischen Reichsanstalt*, 18: 45-52.
- Preto, N. & Hinnov, L.A. (2003): Unravelling the origin of shallow-water cyclothems in the Upper Triassic Dürrenstein Fm. (Dolomites, Italy). – *Journal of Sedimentary Research*, 73: 774-789.
- Preto, N., Roghi, G. and Gianolla, P. (2005): Carnian stratigraphy of the Dogna area (Julian Alps, northern Italy): tessera of a complex palaeogeography. – *Boll. Soc. Geol. It.*, 124: 269-279.
- Ragazzi, E., Roghi, G., Giaretta, A. and Gianolla, P. (2003): Classification of amber based on thermal analysis. – *Thermochimica Acta*, 404 (1-2): 43-54.
- Retallack, G.J. & Royer, D.L. (2000): Depth to pedogenetic carbonate horizon as a paleoprecipitation indicator? Comment and reply. – *Geology*, 28: 572-573.
- Retallack, G.J. (2001): *Soils of the past: an introduction to paleopedology* (2nd edition). – Unwin-Hyman Ltd, London, 404 pp.
- Roghi, G. (2004): Palynological investigations in the Carnian of Cave del Predil area (once Raibl, Julian Alps). – *Review of Paleobotany and Palynology*, 132: 1-35.

- Roghi, G., Kustatscher, E. and van Konijnenburg-van Cittert, J.H.A. (2006a): Late Triassic Plant from Julian Alps (Italy). - *Boll. Soc. Paleont. It.*, 45 (I): 133-140.
- Roghi, G., Ragazzi, E. and Gianolla, P. (2006b): Triassic amber of the Southern Alps (Italy). - *Palaios*, 21: 143-154.
- Rossi, D. (1964): Il Trias medio e superiore nelle Dolomiti nord-orientali. - *Rend. Sc. fis. mat. e nat.*, 37: 322-329.
- Russo, F., Neri, C., Mastrandrea, A. and Laghi, G.F. (1991): Depositional and diagenetic history of the Alpe di Specie (Seelandalpe) fauna (Carnian, northeastern Dolomites). - *Facies*, 25: 187-210.
- Schlager, W. & Schöllnberger, W. (1974): Das Prinzip stratigraphischer Wenden in der Schichtfolge der Nördlichen Kalkalpen. - *Mitt. Geol. Ges.*, 66-67: 165-193.
- Sigmund, A. (1937): Die Minerale Niederösterreichs (2nd ed). - Deuticke, Wien-Leipzig, 247 p.
- Simms, M.J. & Ruffell, A.H. (1989): Synchronicity of climatic change and extinctions in the Late Triassic. - *Geology*, 17: 265-268.
- Schmidt, A., Ragazzi, R., Coppellotti, O. and Roghi, G. (2006): A microworld in 220 million-year-old drops of amber. - *Nature*, 444: 835.
- Soom, M. (1984): Bernstein vom Nordrand der Schweizer Alpen. - *Stuttgarter Beiträge zur Naturkunde, Serie C*, 18: 15-20.
- Stefani, M., Bosellini, A., Brack, P., Gianolla, P., Keim, L. and Preto, N. (2004): Triassic carbonate platforms of the Dolomites (Italy): carbonate production, relative sea-level fluctuations and the shaping of the depositional architecture. - 32nd International Geological Congress, 20-28 agosto, 2004, Firenze.
- Van der Eem, J.G.L.A. (1983): Aspects of Middle and Late Triassic Palynology. 6. Palynological investigations in the Ladinian and Lower Karnian of the Western Dolomites, Italy. - *Rev. Palaeobot. Palynol.*, 39: 189-300.
- Vávra, N. (1984): Reich an armen Fundstellen. - Übersicht über die fossilen Harze Österreichs: *Stuttgarter Beiträge zur Naturkunde, Serie C*, 18: 9-14.
- Wendt, J. & Fürsich, F.T. (1980): Facies analysis and palaeogeography of the Cassian Formation, Triassic, Southern Alps. - *Riv. It. Paleont. Stratigr.*, 85: 1003-1028.
- Zardini, R. (1973): Geologia e fossili attorno a Cortina d'Ampezzo. - Edizioni Ghedina, Cortina d'Ampezzo, 26 pp.

Manuscript submitted: 14.1.2009
Revised manuscript accepted: 6.2.2009